Accepted Manuscript

Late Triassic - Late Jurassic subsidence analysis in Neuquén Basin central area

Nicolas Scivetti, Juan R. Franzese

PII: S0895-9811(19)30080-X

DOI: https://doi.org/10.1016/j.jsames.2019.102230

Article Number: 102230

Reference: SAMES 102230

To appear in: *Journal of South American Earth Sciences*

Received Date: 11 February 2019

Revised Date: 30 May 2019

Accepted Date: 10 June 2019

Please cite this article as: Scivetti, N., Franzese, J.R., Late Triassic - Late Jurassic subsidence analysis in Neuquén Basin central area, *Journal of South American Earth Sciences* (2019), doi: https://doi.org/10.1016/j.jsames.2019.102230.

Late Triassic - Late Jurassic subsidence analysis in Neuquén Basin central area

Nicolas Scivetti[1*], Juan R. Franzese[2].

[1]Instituto Geológico del Sur – CONICET – UNS, San Juan 670, Bahía Blanca, Argentina.

[2]Centro de Investigaciones Geológicas – CONICET – UNLP, Diagonal 113 N°275, La Plata, Argentina.

*Corresponding author: nscivetti@ingeosur-conicet.gob.ar

Abstract

This paper presents a detailed study of the tectonic subsidence evolution during the Late Triassic - Late Jurassic period in the central area of the Neuquén Basin. The methodology consisted of the integration of outcrop and subsurface data, in order to obtain tectonic subsidence curves for the analyzed period in the study area. The origin of the basin was linked to a lithospheric mechanical extension episode in the Late Triassic - Early Jurassic that, once completed, gave rise to a post-rift stage. The post-rift stage, comprised between Early Jurassic and Early Cretaceous, was classically assumed as dominated by thermal subsidence. Results obtained in this paper show that there is a change in the geometry of the tectonic subsidence curves, which depart considerably from the expected behavior for a basin dominated by thermal subsidence. Therefore, the post-rift stage of the Neuquén Basin for the study area would have had a more complex tectonic evolution than that determined exclusively by the thermal subsidence, and that superposition of mechanisms must be considered. From the available data, a shift from thermal to dynamic subsidence from the Middle Callovian onwards seems to be the most plausible explanation for the subsidence evolution observed in the study area.

Keywords: Subsidence analysis; 1D backstripping; Neuquén Basin; Lotena Group; post-rift.

1. Introduction

Even though the Neuquén Basin has been studied extensively for more than a century, both from the scientific and industry point of view (Howell et al., 2005), its tectonostratigraphic evolution is not yet fully understood. Its development begins in the Late Triassic and extends to the Cenozoic, being classically divided into three different stages: syn-rift stage (Late Triassic to Early Jurassic), post-rift stage (Early Jurassic to Early Cretaceous) and foreland stage (Late Cretaceous to Cenozoic) (Legarreta & Uliana, 1996). The post-rift stratigraphic record is characterized by a series of discontinuities and unconformities (Howell et al., 2005). Many of these surfaces were considered as the product of eustatic variations (Legarreta & Gulisano, 1989) however, during this stage various tectonic events have been recognized, which led to consider tectonics as a transcendental control factor over the stratigraphic evolution (Zavala, 1993; Vergani et al., 1995; Fernández Seveso et al., 1996; Limeres, 1996; Burgess et al., 2000; Comínguez & Franzese, 2005; Ramos & Kay, 2006; Mescua et al., 2008; Barredo et al., 2008; Barredo & Stinco, 2010; Spalletti, 2013). This allows supposing that more complex tectonic processes than just the thermal subsidence could have operated during that stage. The stages in which the Neuquén Basin evolution has been divided imply different conditions of subsidence but the published papers about tectonic subsidence in this basin are scarce (Manceda & Figueroa, 1995; Sigismondi, 2012; Horton & Fuentes, 2016). Although the stratigraphy of the post-rift stage is consistent with documented eustatic cycles from a regional point of view, local tectonic factors (Vergani et al., 1995; Vergani, 2005) would have exercised a strong control over the stratigraphic evolution modifying sediment generation and dispersion patterns in the central - western area (Schwarz et al., 2006; Veiga et al., 2011). In addition, the Andean magmatic arc tectonics would have generated regional

slopes, modifying the geometry of the basin during its evolution (Spalletti et al., 2008). The objective of this paper is to analyze the subsidence mechanisms between Late Triassic and Late Jurassic for the central sector, in order to understand the tectonic evolution of the basin during that period. This analysis is based on the pattern variations of the tectonic subsidence curves.

2. Geological setting

The Neuquén Basin is located on the eastern side of the Andes in Argentina and central Chile, between 32° and 40° S (Howell et al., 2005), covering nearly 120.000 km² (Yrigoyen, 1991). It has a roughly triangular shape limited by the North Patagonian Massif to the southeast, the Sierra Pintada System to the northeast and the Andean cordillera to the west (Vergani et al., 1995) (Figure 1). It contains a continuous stratigraphic record of up to 7.000 meters thick accumulated during at least 220 My (Vergani et al., 1995) and has been described as an ensialic depression located in a back-arc position since the Early Jurassic (Legarreta & Uliana, 1996). Its evolution can be divided into three different stages (Howell et al., 2005), which have a close relationship with the processes occurred in the western margin of Gondwana (Uliana et al., 1989; Legarreta & Uliana, 1996; Franzese & Spalletti, 2001; Ramos & Folguera, 2005): I) Initial or rift stage (Late Triassic to Early Jurassic). During the Late Triassic and the Early Jurassic, the Neuquén Basin was affected by an extensional regime (Vergani et al., 1995; Franzese & Spalletti, 2001) in a context of active subduction in the southwestern margin of Gondwana (Oliveros et al., 2015; González et al., 2018). The extensional tectonic regime prevailing during this period has been interpreted as the beginning of the rift stage in the basin (Vergani et al., 1995; Franzese & Spalletti, 2001) and according to this, the stage has been considered to have been controlled by mechanical subsidence with the consequent development of grabens and half-grabens (Figure 2a), with lengths of up to 150 kilometers, widths of 50 kilometers and a thickness of more than 2000 meters (Legarreta & Gulisano, 1989; Uliana et al., 1989; Manceda & Figueroa, 1993; Vergani et al., 1995; Legarreta & Uliana, 1996). The infill includes continental siliciclastic, volcanic and volcaniclastic materials (Gulisano et al., 1984; Franzese et al., 2007; Pángaro et al., 2009;

Muravchik et al., 2011; D'Elia et al., 2012; D'Elia & Martí, 2013) grouped into the Precuyano Cycle (Gulisano et al., 1984). II) Second or post-rift stage (Lower Jurassic to Lower Cretaceous). According to Uliana et al. (1989), Franzese & Spalletti (2001), Ramos & Folguera (2005) and Howell et al. (2005), the post-rift stage was characterized by the predominance of thermal subsidence and the connection of initially isolated depocenters (Figure 2b). At the same time, Jurassic and Early Cretaceous arc magmatism is well exposed in the present-day Coastal Cordillera of Peru and Chile (Rossel et al., 2013) denoting an active subduction for this period. During this stage a succession of marine and continental deposits was accumulated under different paleogeographic scenarios with its thickness controlled by eustatic variations (Legarreta & Gulisano, 1989). III) Third or foreland stage (Late Cretaceous to Cenozoic). Characterized by the disconnection of the previous basin with the proto-Pacific Ocean (Aguirre-Urreta et al., 2008), continental deposits and the predominance of flexural subsidence (Howell et al., 2005) (Figure 2c). The growth of the Andean fold and thrust belt in the western margin of the basin would have generated the deformation and exposure of Mesozoic deposits as well as the inversion of preexisting normal faults (Ramos & Folguera, 2005).

2.1 Study area

The study area is located in the eastern sector of the Neuquén Basin, including the southern sector of the Mendoza province and the northern sector of the Neuquén province in the Argentine territory. This area was defined on the basis of the presence of outcrops and on the availability of subsurface data, allowing a physical correlation of the major stratigraphic units (Figure 3). It is comprised between 36°30' and 37°2 0' south latitude and 69°00' and 69°50' west longitude. It has a quadrangular geometry with sides of approximately 80 kilometers

length, covering about 6400 km^2. Its north-northeast limit corresponds to the Altiplanicie del Payún region, while the south-western limit is represented by the Tromen volcano. The Sierra de Chachahuén constitutes the southeast boundary (Figure 3). The most outstanding morphostructural features within the study area are Sierra de Cara Cura and Sierra de Reyes ranges. Both structures constitute west-vergent anticlines with a north-south orientation, approximately parallel to the Andean chain. The origin of these structures would be associated with Andean reverse faults (Pángaro et al. 2004; Giambiagi et al. 2008; Bechis, 2009).

3. Stratigraphy

The stratigraphic record of the Neuquén Basin contains units belonging to the three stages defined above. The syn-rift stage (Stage I) units were grouped under the Precuyano Cycle and include pyroclastic, volcanic and epiclastic deposits of the initial filling in the Neuquén Basin (Gulisano et al., 1984; Franzese et al., 2007; Pángaro et al., 2009; Muravchik et al., 2011; D'Elia et al., 2012; D'Elia & Martí, 2013). These deposits exceed 2000 meters in thickness and represent almost exclusively continental deposits contained within half-graben structures forming isolated depocenters. The base of the unit is defined by a regional unconformity named the Supratriassic unconformity while the top is limited by the Intraliassic unconformity (Gulisano et al., 1984) (Figure 4). The post-rift stage (Stage II) begins with the Cuyo Group (Sinemurian – Middle Callovian). The Cuyo Group (Dellapé et al., 1978) (Figure 4) represents the beginning of the post-rift stage in the entire Neuquén Basin (Veiga et al., 2013). It is limited at base and top by the Intraliassic and Intracallovian unconformities, respectively. The first one represents the first episode of marine ingression on volcanic deposits of the pre-rift (Stipanicic et al., 1968) and/or deposits of the Precuyano Cycle. The Cuyo Group deposits have a wide variability of facies, thickness and ages, resulting in different lithostratigraphic units (Arregui et al., 2011). A variety of sedimentary environments is also recognized, including deep marine (Los Molles Formation), marine platform (Bardas Blancas Formation), deltaic (Lajas Formation), continental (Challacó Formation), carbonate platform (Chachil Formation) and evaporitic (Tábanos Formation). Covering the Cuyo Group, the Lotena Group (Middle Callovian – Late Oxfordian) (Leanza, 1992) (Figure 4) is limited at the base and top by two unconformities that are called Intracallovian and Intramalmic, respectively (Dellapé et al., 1979; Gulisano et al., 1984). The Lotena Group shows a lesser

thickness and a shorter regional span than the Cuyo Group. The lithostratigraphic units involve continental sandy and platform facies named Lotena Formation (Weaver, 1931), limestone of La Manga Formation (Stipanicic, 1966) and a thick evaporite sequence named Auquilco Formation (Weaver, 1931) (Figure 4). Finally, the uppermost unit of the post-rift stage is the Mendoza Group (Late Oxfordian / Kimmeridgian – Lower Barremian) (Stipanicic & Rodrigo, 1968) (Figure 4). This unit is limited at the base and top by the Intramalmic and Intrabarremian unconformities, respectively. It is composed of Kimmeridgian continental clastic sediments of the Tordillo Formation (Stipanicic, 1966), marls, black shales and lime mudstones of the Vaca Muerta Formation (Late Early Tithonian - Early Valanginian) (Weaver, 1931), continental and marine deposits of the Mulichinco Formation (Early Valanginian - Late Valanginian) (Weaver, 1931) and claystones and limestones of the Agrio Formation (Late Valanginian - Early Barremian) (Weaver, 1931) (Figure 4).

4. Materials and methods

Data used for this paper comes from the stratigraphic record of syn-rift and post-rift stages of the basin (Stages I and II). Some of this data was collected in outcrop while the subsurface data comes from the hydrocarbon industry. Field activities included the delimitation of the formational units and systematic measurements of thickness, dip direction and dip and fractures and faults in 207 points of interest. Furthermore, three stratigraphic logs [Cara Cura Norte (CCN), Cara Cura Sur (CCS) and Reyes Sur (Reyes S)] were described in the study area (Figure 5). The YPF S.A. company delivered subsurface data of reports and well logs of 33 exploration wells (Figure 5). Since the Precuyano Cycle has not petroleum interest in the study area, only three wells (CG x-1, LB x-2 and EP x-3) reach the pre-rift deposits. Therefore, the determination of tectonic subsidence for the syn-rift stage was carried out using these wells together with sedimentological logs described in outcrops and bibliography data (Rossi & Veiga, 1990; Naipauer et al., 2016; Drosina et al., 2017).

4.1 1D backstripping

The backstripping technique (Watts & Ryan, 1976) uses the stratigraphic record to quantitatively estimate the basement (or any other unit) depth in the absence of sediment and/or water loading over time. It applies corrections related to porosity and density of sediments, bathymetry of accumulation and eustatic variations. Plotting these values across time, tectonic subsidence curves can be obtained. In addition, by comparing with theoretical subsidence curves, it is possible to infer the mechanisms of basin formation (Xie & Heller, 2009).

169 This operation was carried out using thickness, depth and lithology data obtained in the field
170 and from subsurface. Values of current porosity, lithology and density were determined from
171 well logs. The effect of sediment decompaction during the backstripping procedure was
172 calculated according to Sclater & Christie (1980) (Table 1). The determination of water depth
173 for a given stratigraphic horizon is generally far from easy. For the same rate of tectonic
174 subsidence, enormously different stratigraphic thicknesses can result, depending on the initial
175 and ensuing paleobathymetry (Allen & Allen, 2005), however for shallow water depths, up to
176 200 m, estimating the water depth is easier and the errors associated are smaller (Holt,
177 2012). In addition, any uncertainties due to water-depth assignments are reduced by working
178 with relatively thick stratigraphic successions (Xie & Heller, 2009). Information on
179 paleobathymetry comes from several sources such as benthic microfossils, other faunal and
180 floral assemblages, sedimentary facies and distinctive geochemical signatures (Allen & Allen,
181 2005). Paleobathymetry values (Table 2) were estimated from biostratigraphic reports
182 (Angelozzi & Ronchi, 1997; Ronchi & Angelozzi, 1998; Kielbowicz, 1992) based in the study
183 of calcareous microfossils, calcareous nannofossils and carbonaceous microfossils.
184 Estimations from sedimentary data were based in the sedimentary structures given that they
185 are restricted to a particular depth and quantitative techniques are available to constrain the
186 depth at which were formed (Allen, 1984; Immenhauser, 2009). For each unit, it is possible to
187 provide a palaeo-water depth uncertainty range (Berra & Carminati, 2010). Within these
188 ranges, we used the mean or the most likely bathymetry value. The use of different values of
189 palaeo-water depth (maximum, minimum and mean value) results in changes for the
190 calculated subsidence magnitude, but the geometry of the subsidence curves is the same
191 (Figure 6). Ages assigned to the units (Table 3) consist of approximations based on

bibliographic data collection (Franzese & Spalletti, 2001; Schwarz, 2003; Aguirre Urreta et al., 2008; Palma & Kietzmann, 2008; Schiuma & Llambías, 2008; Kamo & Riccardi, 2009; Spalletti et al., 2010; Arregui et al., 2011; Leanza et al., 2011; Spalletti et al. 2011; Naipauer, 2012, 2015). The use of eustatic level variation values from global eustatic curves is not a reliable procedure and currently there is no consensus about its validity. Not only absolute eustatic movements determine the height of sea level, but also local tectonic factors condition the position of coastline (Kominz, 2001). Estimations made on a large temporal scale have a greater probability to represent reality (Watts, 2001), but anyway can introduce a considerable error in subsidence analysis. Therefore, in this paper, we decided not to apply the eustatic sea level correction. Currently, 1D backstripping technique can be carried out using different programs. The one used in this paper was *Backstrip* (Cardozo, 2015) which was compiled to perform 1D Airy backstripping with exponential porosity reduction. This program allows setting values of thickness, bathymetry, eustatic level and porosity of units to obtain uncompacted thickness sediment load corrected and tectonic subsidence curves in graphic and numerical form.

4.2 Lithosphere flexure

The long-term lithospheric response to geological loads can be satisfactorily modeled as an elastic plate overlaying a weak substratum (Watts et al., 1982). While the flexural strength of the lithosphere is strictly defined by its flexural rigidity (D) that it is commonly expressed in terms of another variable, the effective elastic thickness (Te):

$$\mathrm{D} = \frac{E\,Te^3}{12\,(1\,-v^2)}$$

where E is Young's modulus and v is Poisson's ratio. The effective elastic thickness is a notional parameter which describes the thickness of a perfectly-elastic layer with the same flexural strength as the lithosphere (Roberts et al., 1998). The differential equation used to obtain the plate deformation in some point of it is given by:

$$\mathrm{D}\,\frac{d^4w(x)}{dx^4} + (\rho m - \rho i)gy(x) = P(x)$$

where x is the distance along the surface before deformation, y is the deformation, ρm is the average density of the asthenospheric mantle, ρi is the average density of the infill material and g is the gravity acceleration value (Choudhuri & Nemčok, 2017). The software used in this work to obtain the lithospheric flection was *Flex2D* (Cardozo, 2016) which allows visualizing, in plots and tables, the deformation profile produced by geological loads.

5. Results

1D backstripping technique was applied to wells and stratigraphic logs. Resulting tectonic subsidence curves are presented in Figure 7. Classically, deposits associated with the thermal subsidence stage of Neuquén Basin are assumed to be composed by Cuyo, Lotena and Mendoza groups. However, tectonic subsidence patterns obtained in all curves show an upwards convex geometry since the beginning of Lotena Group to the beginning of Mendoza Group, indicating acceleration in the tectonic subsidence. This pattern differs absolutely from the one expected for a purely extensional basin dominated by periods of mechanical and thermal subsidence and it means that the basin was not characterized by cooling of a pure extensional regime as the one that controls the rifting in an intracratonic area.

6. Discussion

Currently, there is a broad consensus about the extensional origin of the Neuquén Basin (Vergani et al.,1995; Franzese & Spalletti, 2001). Both in subsurface as well as in outcrops, grabens and half-grabens can be recognized with more than 2000 meters of sediments infill (Cristallini et al., 2009). The post-rift stage would have begun in Hettangian or Pliensbachian times and would have extended up to the Early Cretaceous. However, subsidence curves obtained in this stage show substantial differences with those expected for a basin under thermal subsidence (Figure 8). In all analyzed wells and stratigraphic logs, the tectonic subsidence curves depart from the theoretical evolution of extensional basins and show a similar geometric pattern. The geometric description by intervals of the tectonic subsidence curves can be done as follows (Figure 8):

1) Initial interval with a linear and high negative slope.

2) Interval from horizontal to slightly upwards concavity and asymptotic tendency.

3) Interval with convex upwards geometry.

The interval 1 (200 - 190 My) shows a linear geometry and high negative slope (Figure 8). These particularities are characteristic of mechanical extension episodes (Allen & Allen, 2005), with fast accommodation space generation rate by means of normal faulting structures (grabens and half-grabens). This interval represents the syn-rift stage of the basin, during which the Precuyano Cycle accumulated.

The interval 2 (190 -164.6 My) shows a slightly upwards concave geometry, during which the Cuyo Group accumulated. In conjunction with the interval 1, they would form the typical geometry for basins with an extensional origin (Allen & Allen, 2005) in which a high

subsidence generation rate is followed by a long period of thermal subsidence with upwards concave geometry (McKenzie, 1978).

The interval 3 (164.6 to 153 My) presents an upwards convex geometry and represents the interval of Lotena Group accumulation (Figure 8). The upwards convex geometry in tectonic subsidence curves is associated with basins dominated by the flexure of the lithosphere (Allen & Allen, 2005). In this interval, subsidence departs from the thermal subsidence behavior observed towards the end of the Cuyo Group. Furthermore, tectonic subsidence shows an increasing rate. This means that the beginning of the Lotena Group would be marked by a change in the dominant subsidence mechanism.

6.1 Tectonostratigraphic analysis

The tectonostratigraphic analysis consists in the study of relationships between large lithostratigraphic units and tectonic settings at the time of their accumulation (Watkinson et al., 1977). A tectonostratigraphic unit comprises all lithostratigraphic units accumulated under the same tectonic conditions and may include one or more chronostratigraphic units. Following, a tectonostratigraphic analysis will be carried out based on the interpretation and association of tectonostratigraphic units.

1. Extensional basin stage: This stage includes Interval 1 and 2 of the tectonic subsidence curves (Figure 8), which are consistent with the expected behavior for the McKenzie extensional model (1978), even in a context of active subduction in the southwestern margin of Gondwana (Oliveros et al., 2015; González et al., 2018). This model predicts an asymptotic decrease in thermal subsidence after an episode of extension of the lithosphere (Joy, 1993). Within this framework, the Precuyano Cycle

277 can be considered as composed by deposits associated with the extensional stage of
278 the basin. The Cuyo Group can be described as a shallowing supersequence that
279 begins with a flood event over the Precuyano Cycle deposits and ends with the
280 continentalization of the deposits in the Middle Callovian (Legarreta & Uliana, 1996;
281 Arregui et al, 2011). This vertical arrangement is consistent with the geometry
282 expected for a thermal subsidence stage, in which basins progressively lose the
283 capacity to generate accommodation space. The stratigraphic evolution of the Cuyo
284 Group in the study area, represented by Los Molles, Lajas and Bardas Blancas
285 formations, could represent the progradation of shallow accumulation systems that fill
286 up the basin.

287 2. Flexural stage: This stage corresponds to interval 3 of the tectonic subsidence curves
288 (Figure 8). It involves Lotena, La Manga and Auquilco formations, forming the Lotena
289 Group. The upwards convex geometry of the tectonic subsidence curves for this
290 interval means that exists an acceleration in the subsidence generation rate, thus it
291 could be thought that the accumulation of the Lotena Group was controlled by a
292 flexural subsidence mechanism (Allen & Allen, 2005). More representative flexural
293 dominated basins are known as foreland basins, which is the case of Andean retroarc
294 basins (Ramos, 1978; DeCelles & Giles, 1996; Franzese et al., 2003, 2011; D'Elía et
295 al., 2016). However, characteristics of the subsidence curves of this interval in the
296 study area do not allow us to classify this stage as a foreland basin, because they do
297 not agree with the "Duration of subsidence / Tectonic subsidence rate" ratio
298 established for this kind of basins (Allen & Allen, 2005). The infill thickness of the
299 foreland basins reaches tenths of kilometers (Allen & Allen, 2005), while the Lotena

Group in the study area reaches a maximum of 200 meters. Even in depocentral sectors of the Neuquén Basin it reaches about 1000 meters thick (Arregui et al., 2011). Foreland basins have a duration between 20 and 80 million years and a maximum rate of subsidence generation between 0.05 and 0.5 mm/y (Naylor & Sinclair, 2008; Sinclair, 2012), while the Lotena Group has a duration of about 11 million years and, for the study area, it has a subsidence generation rate one order of magnitude less than the aforementioned minimum. On the other hand, discontinuities within the Lotena Group have not been documented, as well as other characteristics of foreland basin deposits. For the Callovian - Oxfordian period there is evidence of a growth of a volcanic arc in the current Chilean Cordillera de la Costa (Figure 1), which would have acted as a source of clastic and volcanic material during that period (Charrier et al., 2007; Nasi, 2010). As it has been demonstrated, the load produced by the height growth of volcanic buildings over the lithosphere can cause its flexure (Collier & Watts, 2001; Turcotte & Schubert, 2002). Therefore, the mentioned volcanic arc could have generated the flexural subsidence that allowed the accumulation of the Lotena Group. The hypothesis that the load generated by volcanism in the Cordillera de la Costa could generate the subsidence observed for this period was tested. For this, the lithospheric flexure produced by a volcanic arc was calculated. The load was set with a density of 2700 Kg / m³, over a lithosphere with an estimated elastic thickness of 5, 10 and 25 kilometers [although values close to 5 km should be as expected for a rift basin once finished the extension episode (Watts, 2001), and current values are close to 10 km in Chos Malal area (Sigismondi, 2012) (Figure 1)], and was located 250 kilometers away from the study area. The results indicate that it is not possible to generate the

subsidence observed in the study area regardless the height of the load. Loads of 500, 1000 and 1500 meters in height, only produce different subsidence values close to the load, but in none case they generate vertical movements in the study area (Figure 9). Furthermore, the volcanic arc was also active during the deposition of the Cuyo Group (Vergara et al.,1995; Charrier et al., 2007) with no influence on the subsidence during its accumulation. Therefore, this hypothesis was ruled out. Another possible mechanism would correspond to the slow flexure. The slow flexure response has been described as exponentially positive (Thorne & Watts, 1989). It is commonly associated with strike-slip faulting of varying magnitudes, depending on proximity to the driving force (Williams, 1995). Although the existence of strike-slip faulting systems for the Neuquén Basin has been recognized (Mosquera et al., 2006), the time involved to generate this kind of subsidence pattern is much greater than the observed for the accumulation of Lotena Group. Also, strike-slip faulting cannot be demonstrated in all basins where this curve type is seen. Thus, the slow flexure mechanism could be discarded. Another relevant event for the Neuquén Basin was the uplift of the Huincul High (Figure 1). This structure of 300 kilometers in length with an east-west orientation was the result of the intraplate deformation associated with the convergent margin. The Jurassic - Tertiary tectonic activity of the Huincul High controlled the sedimentation in the south of the Neuquén Basin (Mosquera et al., 2011) and its uplift produced the erosion of up to 2000 meters of deposits (Orchuela & Ploszkiewicz, 1984; Ploszkiewicz et al., 1984; Legarreta & Uliana, 1996). Several episodes of Jurassic - Cretaceous deformation have been recognized in the Huincul High region (Bettini, 1984; Zavala, 1993; Vergani et al., 1995) which would have begun in the Early

346 Jurassic (Vergani et al., 1995; Gómez Omil et al., 2002) with major uplift events in the
347 Toarcian, Kimmeridgian and Valanginian (Silvestro & Zubiri, 2008). In the same way
348 that the Cordillera de la Costa, the height and distance of the Huincul High (emplaced
349 over a lithosphere with the aforementioned characteristics) along with its uplift
350 chronology are not consistent with an important flexural subsidence during the
351 Callovian. Therefore, the Huincul High uplift could not have exerted an important
352 control over the subsidence during the Late Callovian - Late Oxfordian period in the
353 study area. At the same time, it should be considered that more than one subsidence
354 mechanism may be acting simultaneously during basin evolution. This situation is
355 common in Andean type convergent boundaries (Allen & Allen, 2005). In these
356 regions, the dynamic topography associated with the subduction of an oceanic
357 lithosphere acts in a significant way (Painter, 2013) and its influence could extend
358 more than 1000 kilometers from the trench towards the interior of the continent (Allen
359 & Allen, 2005). Therefore, the hypothesis that the action of the dynamic subsidence
360 associated with the subduction in the southwestern margin of Gondwana could have
361 generated the lithospheric flexure that allowed the accumulation of Lotena Group was
362 tested. The measurement of dynamic topography behind trenches is problematic,
363 since the dynamic topography must be separated from other forms of subsidence. A
364 first approach to the estimation of dynamic topography behind ancient subduction
365 zones is to use an expression for the geometric form by assuming that it is made of
366 two components: (i) an exponential component with an exponent λ and maximum
367 deflection fm; and (ii) a linear tilt with a maximum gradient α in m km^{-1} and a

368 maximum distance from the trench at which tilting occurs η. Combining these
369 components gives:

$$f(x) = fm\ (e^{-x/\lambda}) + \ \alpha(\eta - x)$$

370 where x is the horizontal orthogonal distance from the trench (Allen & Allen, 2005).
371 Using different parameters, we can obtain the dynamic topography values (Figure 10).
372 Considering that the study area was located 400 kilometers away from the subduction
373 zone, the dynamic topography calculated using fm = 500 km, λ = 200 km, α = 0.2, and
374 η = 1000 km is consistent with the subsidence values obtained for the Lotena Group.
375 Therefore, the dynamic topography associated with the subduction in the southwestern
376 margin of Gondwana could have been the principal subsidence mechanism from
377 Middle Callovian to Late Oxfordian.
378
379

7. Conclusions

Based on results and discussion presented in this paper, it is proposed that Late Triassic - Late Jurassic tectonic evolution of the Neuquén Basin for the study area has two clearly differentiated stages. An initial one, between Late Triassic - Early Jurassic and Middle Callovian with characteristics of extensional basin. In this stage, the Precuyano Cycle tectonostratigraphic unit would represent deposits accumulated during a mechanical extension episode and the Cuyo Group tectonostratigraphic unit would represent those accumulated during thermal subsidence domain. The tectonic subsidence curves for this stage present a good fit with theoretical and empirical models for this kind of basins, even in an active subduction context for the southwest margin of Gondwana. So, strictly, only the Cuyo Group deposits would constitute the post-rift deposits of the Neuquén Basin in the study area. From Middle Callovian to Late Oxfordian, a second stage would have started due to the influence of the dynamic topography associated with the subduction of oceanic lithosphere beneath the southwestern Gondwana margin. During this stage, the lithospheric tilting would have been the predominant subsidence mechanism.

Acknowledgments

Authors manifest their gratitude to CONICET and UNLP for funding this work. Also, to the Subsecretaría de Energía y Minería de la Provincia de Mendoza; the Subsecretaría de Energía, Minería e Hidrocarburos de la Provincia de Neuquén and YPF Company for the access to subsurface data. Finally, to the reviewers Dr. J. Mescua, Dr. V. Ramos and Dr. R. Charrier, who helped to improve the quality of this work and to Dr. Agustín Argüello Scotti and Dr. Luciano Zapata for their collaboration in field activities and critical suggestions on early versions of the manuscript.

406 **References**

407 Aguirre-Urreta, M. B., Pazos, P. J., Ramos, V. A., Ottone, E. G., Laprida, C. & Lazo, D. G.
408 (2008). The Pichaihue Limestones (Late Cretaceous) in the Agrio fold and thrust belt,
409 Neuquén Basin, Argentina. En *7th International Symposium on Andean Geodynamics*
410 *(ISAG 2008, Nice), Extended Abstracts* (pp. 33-36).

411 Allen, P. A. (1984). Reconstruction of ancient sea conditions with an example from the Swiss
412 Molasse. Marine Geology, 60(1-4), 455–473.

413 Allen, P. A. & Allen, J. R. (2005). *Basin analysis: Principles and application to petroleum play*
414 *assessment*. *Second Edition*. Wiley – Blackwell, Hoboken, New Jersey, 560 p.

415 Angeolozzi, G. & Ronchi, D. (Unpublished results, 1997). Estudio bioestratigráfico del pozo
416 YPF.Nq.ECh x-1. YPF.

417 Arregui, C., Carbone, O. & Martínez, R. (2011). El Grupo Cuyo (Jurásico Temprano-Medio)
418 en la Cuenca Neuquina. In: *Geología y Recursos Naturales de la Provincia del*
419 *Neuquén. Relatorio del XVIII Congreso Geológico Argentino* (pp. 77-89). Neuquén,
420 Argentina.

421 Barredo, S., Cristallini, E., Zambrano, O., Pando, G. & García, R. (2008). Análisis
422 tectosedimentario del relleno de edad precuyana y cuyana inferior de la región
423 septentrional del alto de Kauffman, Cuenca Neuquina. VII Congreso de Exploración y
424 Desarrollo de Hidrocarburos, Trabajos Técnicos: 443-455.

425 Barredo, S. & Stinco, L. (2010). Geodinámica de las cuencas sedimentarias: su importancia
426 en la localización de sistemas petroleros en la Argentina. *Petrotecnia, 2*, 48-68.

427 Bechis, F. (2009). Deformación transtensiva de la cuenca Neuquina: Análisis a partir de
428 ejemplos de campo y modelos análogos. Tesis doctoral, Universidad de Buenos Aires
429 (inédita), 264 pp., Buenos Aires.

430 Berra, F. & Carminati, E. (2010). Subsidence history from a backstripping analysis of the
431 Permo-Mesozoic succession of the Central Southern Alps (Northern Italy). *Basin*
432 *Research*, *22*(6), 952-975.

433 Bettini, F. H. (1984). Pautas sobre cronología estructural en el área del cerro Lotena, cerro
434 Granito y su implicancia en el significado de la dorsal del Neuquén, provincia de
435 Neuquén. *IX Congreso Geológico Argentino*, Buenos Aires, II, 342-361.

436 Burgess, P M., Flint, S. & Johnson, S. (2000). Sequence stratigraphic interpretation of
437 turbiditic strata: An example from Jurassic strata of the Neuquén basin, Argentina.
438 *Geological Society of America Bulletin, 112*(11), 1650-1666.

439 Cardozo, N. (2015). *Backstrip*. (4.4) [Software]. Stavanger: Universitetet Stavanger.
440 Retrieved from http://www.ux.uis.no/~nestor/work/programs.html.

441 Cardozo, N. (2016). *Flex 2D* [Software]. Stavanger: Universitetet Stavanger. Retrieved from
442 http://www.ux.uis.no/~nestor/work/programs.html.

443 Charrier, R., Pinto L. & Rodríguez M.P. (2007). Tectono-stratigraphic evolution of the Andean
444 orogen in Chile. En: W. Gibbons, y T. Moreno (eds.), *Geology of Chile*, *Chapter 3. The*
445 *Geological Society, London, Special Publication*. 21-116.

446 Choudhuri, M., & Nemčok, M. (2017). *Mantle Plumes and Their Effects* (pp. 1-137). Springer
447 International Publishing.

448 Collier, J.S. & Watts, A.B. (2001) Lithospheric response to volcanic loading by the Canary
449 Islands: constraints from seismic reflection data in their flexural moat. *Geophysical*
450 *Journal International*, *147*(3), 660-676.

451 Comínguez, A. H. & Franzese, J.R. (2005). The deep seismic structure of the central
452 Neuquén Basin, Argentina. *6th International Symposium on Andean Geodynamics*.
453 Barcelona, España. Extended Abstracts: 178-181.

454 Cristallini, E., Tomezzoli, R., Pando, G., Gazzera, C., Martínez, J.M., Quiroga, J., Buhler, M.,
455 Bechis, F., Barredo, S. & Zambrano, O. (2009). Controles precuyanos en la estructura
456 de la cuenca Neuquina. *Revista de la Asociación Geológica Argentina 65* (2): 248-264.

457 DeCelles, P. G. & Giles, K. A. (1996). Foreland basin systems. *Basin Research, 8*(2), 105–
458 123.

D'Elia, L., Muravchik, M., Franzese, J.R, & Bilmes, A. (2012). Volcanismo de sin-rift de la Cuenca Neuquina, Argentina: relación con la evolución Triásico Tardío-Jurásico Temprano del margen Andino. *Andean geology*, *39*(1), 106-132.

D'Elia, L. & Martí, J. (2013). Caldera events in a rift depocentre: an example from the Jurassic Neuquén basin, Argentina. *Journal of the Geological Society, 170*(4), 571-584.

D´Elia, L., Bilmes, A., López, M., Bucher, J., García, M., Hernandez, M., Scivetti, N., Monti, M., Funes, D. & Franzese, J.R. (2016). Tectónica y sedimentación en el patagonian broken foreland a los 40°s: controles externos y p erspectivas futuras para el análisis de cuencas de antepaís. Libro de Resúmenes del VII Congreso Latinoamericano de Sedimentología y XV Reunión Argentina de Sedimentología, p 68. Santa Rosa, La Pampa.

Dellapé, D.A., Pando, G.A., Uliana, M.A. & Musacchio, E.A. (1978). Foraminíferos y ostrácodos del Jurásico en las inmediaciones del arroyo Picún Leufú y la ruta 40 (Provincia del Neuquén, Argentina) con algunas consideraciones sobre la estratigrafía de la Formación Lotena. *VII Congreso Geológico Argentino*, Actas *2*, 489-507. Buenos Aires.

Dellapé, D. A., Pando, G. A., Uliana, M. A. & E. A. Musacchio, (1979). Foraminíferos y ostrácodos del Jurásico en las inmediaciones del arroyo Picún Leufú y la Ruta 40 (provincia de Neuquén, Argentina), con algunas consideraciones sobre la estratigrafía de la Formación Lotena. VII Congreso Geológico Argentino. Neuquén. Actas II: 489-507. Buenos Aires.

Drosina, M., Barredo, S., Martínez, A., & Giambiagi, L. (2017). Facies volcaniclásticas del Ciclo Precuyano en el sector norte de la Sierra de la Cara Cura, Mendoza. Revista de la Asociación Geológica Argentina, 74(2), 179-190.

Fernández Seveso, F, Laffitte, G.A. & Figueroa, D. (1996). Nuevos plays jurásicos en el engolfamiento neuquino, Argentina. *XIII Congreso Geológico Argentino y III Congreso de Exploración de Hidrocarburos*. Actas I: 281 pp.

Franzese, J. R. & Spalletti, L. A. (2001). Late Triassic–early Jurassic continental extension in southwestern Gondwana: tectonic segmentation and pre-break-up rifting. *Journal of South American Earth Sciences*, *14*(3), 257-270.

Franzese, J.; Sapalletti, L.A., Gómez Pérez, I.; Macdonald, D.I.M.; (2003). Tectonic and Paleoenvironmental Evolution of Mesozoic Sedimentary Basins along the Argentinian Andes Foothills (32° - 54° S.L.). Journal of South American Earth Sciences, 16 (2003) 81–90

Franzese, J.R., Veiga, G.D., Muravchik, M., Ancheta, M.D. & D´Elía, L. (2007). Estratigrafía de "sin-rift" (Triásico Superior-Jurásico Inferior) de la Cuenca Neuquina en la Sierra de Chacaico, Neuquén, Argentina. *Revista Geológica de Chile*, *34*(1), 49-62.

Franzese, J R., D'Elia, L., Bilmes, A., Muravchik, M. & Hernández, M. (2011). Superposición de cuencas extensionales y contraccionales oligo-miocenas en el retroarco andino norpatagónico: la Cuenca de Aluminé, Neuquén, Argentina. *Andean Geology, 38*(2), 319-334.

Giambiagi, L., Bechis, F., Barredo, S., & Tunik, M. (2008). Cinemática de la apertura de los depocentros Atuel y Cara Cura-Reyes, Cuenca Neuquina: Rift con múltiples sets de fallas. In: *Congreso de Exploración y desarrollo de Hidrocarburos* (No. 7, pp. 431-442).

Gómez Omil, R., Schmithalter, J., Cangini, A., Albariño, L. & Corsi, A. (2002). El Grupo Cuyo en la Dorsal de Huincul, Consideraciones Estratigráficas, Tectónicas y Petroleras. Cuenca Neuquina. *V Congreso de Exploración y Desarrollo de Hidrocarburos*. Mar del Plata, 22 p.

González, J., Oliveros, V., Creixell, C., Velásquez, R., Vásquez, P., & Lucassen, F. (2018). The Triassic magmatism and its relation with the Pre-Andean tectonic evolution: Geochemical and petrographic constrains from the High Andes of north central Chile (29°30′–30° S). *Journal of South American Earth Sciences*, *87*, 95-112.

Gulisano, C.A., Gutierrez Pleimling, A.R., & Digregorio, R.E. (1984). Esquema estratigráfico de la secuencia jurásica del oeste de la provincia del Neuquén. *IX Congreso Geológico Argentino*, San Carlos de Bariloche, Rio Negro, Argentina, Actas *1*, 236 259.

Holt, P. (2012). *Subsidence Mechanisms of Sedimentary Basins Developed over accretionary Crust.* Doctoral thesis. Durham University, England. http://etheses.dur.ac.uk/3584/.

516 Horton, B. & Fuentes, F. (2016). Sedimentary record of plate coupling and decoupling during
517 growth of the Andes. *Geology*, *44*(8), 647-650.

518 Howell, J. A., Schwarz, E., Spalletti, L. A., & Veiga, G. D. (2005). The Neuquén basin: an
519 overview. *Geological Society, London, Special Publications*, *252*(1), 1-14.

520 Immenhauser, A. (2009). Estimating palaeo-water depth from the physical rock record. Earth-
521 Science Reviews, 96(1-2), 107–139.

522 Joy, A. M. (1993). Comments on the pattern of post-rift subsidence in the Central and
523 Northern North Sea Basin. *Geological Society, London, Special Publications, 71*(1),
524 123-140.

525 Kamo, S.L. & Riccardi, A.C. (2009). A new U–Pb zircon age for an ash layer at the
526 Bathonian–Callovian boundary, Argentina. *GFF*, *131*, 177–182.

527 Kielbowicz, A. (Unpublished results, 1992). Microfósiles calcáreos del pozo YPF.MdN.AN x-2.
528 YPF.

529 Kominz, M. A. (2001). Sea Level Variations over Geologic Time. Encyclopedia of Ocean
530 Sciences, 2605–2613.

531 Leanza, H.A. (1992). Estratigrafía del Paleozoico y Mesozoico anterior a los Movimientos
532 Intermálmicos en la comarca del Cerro Chachil, provincia del Neuquén, Argentina.
533 *Revista de la Asociación Geológica Argentina, 45* (3-4), 272-299.

534 Leanza, H.A., Sattler, F., Martinez, R. & Carbone, O. (2011). La Formación Vaca Muerta Y
535 Equivalentes (Jurásico Tardío-Cretácico Temprano) En La Cuenca Neuquina. En
536 *Geología y Recursos Naturales de la Provincia del Neuquén. Relatorio del XVIII*
537 *Congreso Geológico Argentino* (pp. 113-129). Neuquén, Argentina.

538 Legarreta, L., & Gulisano, C. A. (1989). Análisis estratigráfico secuencial de la Cuenca
539 Neuquina (Triásico superior-Terciario inferior). In: *Cuencas sedimentarias argentinas*
540 (Vol. 6, pp. 221-243). San Miguel de Tucumán: Universidad Nacional de Tucumán.

Legarreta, L. & Uliana, M. A. (1996). The Jurassic succession in west-central Argentina: stratal patterns, sequences and paleogeographic evolution. *Palaeogeography, Palaeoclimatology, Palaeoecology*, *120*(3-4), 303-330.

Limeres, M., (1996). Sequence stratigraphy of the Lower-Middle Jurassic in southwestern Neuquen: implicance of unraveling synsedimentary tectonics along the Huincul wrench system. In A.C. Riccardi (ed.), *Advances in Jurassic Research*. GeoReserch Forum *1-2*: 275-284.

Manceda, R. & Figueroa, D. (1993), La inversión del rift mesozoico en la faja fallada y plegada de Malargüe, Provincia de Mendoza. *XII Congreso Geológico Argentino y II Congreso de Exploración de Hidrocarburos, 3*, 219–232.

Manceda, R. & Figueroa, D. (1995). Inversion of the Mesozoic Neuquén rift in the Malargüe fold-thrust belt, Mendoza, Argentina. En A.J. Tankard, R. Suárez, y H.J. Welsink (eds), *Petroleum Basins of South America, American Association of Petroleum Geologists*, *Memoir* (*62*: 369-382). Mendoza, Argentina.

McKenzie, D. (1978). Some remarks on the development of sedimentary basins. *Earth and Planetary science letters*, *40*(1), 25-32.

Mescua, J. F., Giambiagi, L. B. & Bechis, F. (2008). Evidencias de tectónica extensional en el Jurásico Tardío (Kimeridgiano) del suroeste de la provincia de Mendoza. *Revista de la Asociación Geológica Argentina, 63*(4), 512-519.

Mosquera, A., Ramos, V. A., & Kay, S. M. (2006). Intraplate deformation in the Neuquén Embayment. *Special Papers-Geological Society Of America*, *407*, 97.

Mosquera, A., Silvestro, J., Ramos, V. A., Alarcón, M. y Zubiri, M. (2011). La estructura de la Dorsal de Huincul. Relatorio Geología y Recursos Naturales de la provincia del Neuquén, 385-397. Buenos Aires.

Muravchik, M., D'Elia, L., Bilmes, A. & Franzese, J.R. (2011). Syn-eruptive/inter-eruptive relations in the syn-rift deposits of the Precuyano Cycle, Sierra de Chacaico, Neuquén Basin, Argentina. *Sedimentary Geology 238* (1-2): 132-144.

568 Naipauer, M., García, E., Marques, J., Tunik, M., Rojas, E., Vujovich, G., Pimentel, M. &
569 Ramos, V.A. (2012). Intraplate Late Jurassic deformation and exhumation in western
570 central Argentina: Constraints from surface data and U-Pb detrital zircon ages.
571 *Tectonophysics 524-525*: 59-75.

572 Naipauer, M., Tapia, F., Mescua, J., Farías, M., Pimentel, M. M., & Ramos, V. A. (2015).
573 Detrital and volcanic zircon U–Pb ages from southern Mendoza (Argentina): An insight
574 on the source regions in the northern part of the Neuquén Basin. *Journal of South*
575 *American Earth Sciences, 64*, 434-451.

576 Naipauer, M., Fennell, L., Folguera, A., Pimentel, M., & Ramos, V. (2016). Edades U-Pb
577 SHRIMP de volcanitas del Ciclo Precuyano: controles temporales en la extensión del
578 depocentro Cara Cura-Reyes (36 30'ls), norte de la Cuenca Neuquina. *I Simposio de*
579 *Tectónica Sudamericana*.

580 Nasi, C. & Thiele, R. (1982). Estratigrafia del Jurasico y Cretacico de la Cordillera de la
581 Costa, al sur del rio Maipo, entre Melipilla y Laguna de Aculeo (Chile central). *Revista*
582 *Geológica de Chile,* 16, 81-99.

583 Naylor, M. & Sinclair, H.D. (2008). Pro-versus retro-foreland basins. *Basin Research*, 20,
584 285–303.

585 Oliveros, V., Vásquez, P., Creixell, C., González, J., Espinoza, M., Lucassen, F., & Ducea, M.
586 N. (2015). Lithospheric loss in the Andean convergent margin during the Triassic:
587 geochemical evidence from igneous rocks of northern Chile (24 30'–30 00'S). In *XIV*
588 *Congreso Geológico Chileno*.

589 Orchuela, I. & Ploszkiewicz, V. (1984). La Cuenca Neuquina. In Ramos, V. A. (ed.) Geología
590 y Recursos Naturales de la Provincia de Río Negro. IX Congreso Geológico Argentino.
591 San Carlos de Bariloche, Relatorio, 163-188, Buenos Aires.

592 Painter, C. & Carrapa B. (2013). Flexural versus dynamic processes of subsidence in the
593 North American Cordillera foreland basin. *Geophysical Research Letters, 40*, 1-5.

Palma, R.M. & Kietzmann, D.A. (2008). Ciclos de somerización en facies peritidales de la Formación La Manga: tipos, origen y controles. *XII Reunión Argentina de Sedimentología*. *133,* Buenos Aires.

Pángaro, F., Pereira, M., & Giorgetti, M. (2004). Relevamiento Geológico del Precuyano en las Sierras de Reyes y Cara Cura, Provincia de Mendoza, Argentina. Repsol-YPF (informe inédito).

Pángaro, F., Pereira, D.M. & Micucci, E. (2009). El sinrift del ámbito de la dorsal de Huincul, Cuenca Neuquina: su evolución y control sobre el registro estratigráfico del Jurásico y la evolución estructural del área. *Revista de la Asociación Geológica Argentina 65*: 265-277.

Ploszkiewicz, J. V., Orchuela, I. A., Vaillard, J. C. y Viñes, R. F. (1984). Compresión y desplazamiento lateral en la zona de Falla Huincul: estructuras asociadas, provincia del Neuquén. *IX Congreso Geológico Argentino*, 2, 163-169. Buenos Aires.

Ramos, V.A. (1978). Estructura. En: Rolleri, E.O. (ed.) *Geología y recursos naturales de la Provincia del Neuquén, VII Congreso Geológico Argentino (Neuquén)*, Relatorio 9-24. Buenos Aires.

Ramos, V. A. & Folguera, A. (2005). Tectonic evolution of the Andes of Neuquén: constraints derived from the magmatic arc and foreland deformation. En G. D. Veiga, L. A. Spalletti, J. A. Howell, E. Schwarz (eds.), *The Neuquén Basin: A case study in sequence stratigraphy and basin dynamics. Geological Society, London, Special Publications*, *252*(1), 15-35.

Ramos, V. A. & Kay, S. M. (2006). Overview of the tectonic evolution of the southern Central Andes of Mendoza and Neuquén (35–39 S latitude). *Geological Society of America, Special Paper*,*407*, 1-18.

Roberts, A. M., Kusznir, N. J., Yielding, G., & Styles, P. (1998). 2D flexural backstripping of extensional basins; the need for a sideways glance. *Petroleum Geoscience*, *4*(4), 327-338.

Ronchi, D. & Angeolozzi, G. (Unpublished results, 1998). Estudio bioestratigráfico sobre corona del pozo YPF.Nq.BjDC x-1. YPF.

Rossel, P., Oliveros, V., Ducea, M. N., Charrier, R., Scaillet, S., Retamal, L., & Figueroa, O. (2013). The Early Andean subduction system as an analog to island arcs: Evidence from across-arc geochemical variations in northern Chile. *Lithos*, *179*, 211-230.

Rossi, G. & Veiga, R. (1990). Evaluación estratigráfica, estructural y posibilidades petroleras de la Sierra de Reyes, Provincia de Mendoza. Gerencia General de Exploración, YPF Inédito.

Sawyer, D. S.; Swift, B. A.; Sclater J. G. & Toksöz, M. N. (1982). Extensional model for the subsidence of the northern United States Atlantic continental margin. Geology, 10 (3): 134-140.

Schiuma, M. & Llambías, E.J. (2008). New ages and chemical analysis on Lower Jurassic volcanism close to the Huincul High, Neuquén. *Revista de la Asociación Geológica Argentina, 63*(4): 644-652.

Schwarz, E. (2003). *Análisis paleoambiental y estratigrafía secuencial de la Formación Mulichinco en el sector septentrional de la provincia del Neuquén, Cuenca Neuquina,* Argentina (Tesis de Doctorado). Universidad Nacional de La Plata. La Plata, Argentina. 303 pp. Inédita.

Schwarz, E., Spalletti, L.A. & Howell, J. (2006). Sedimentary response to a tectonically induced sea-level fall in a shallow back-arc basin: the Mulichinco Formation (Lower Cretaceous), Neuquén Basin, Argentina. *Sedimentology, 53*, 55–81.

Sclater, J. G. & Christie, P. A. F. (1980), Continental stretching: An explanation of the Post-Mid-Cretaceous subsidence of the central North Sea Basin, *Journal of Geophysical. Research. 85(B7),* 3711–3739.

Sigismondi, M. E. (2012). Estudio de la deformación litosférica de la cuenca Neuquina: estructura termal, datos de gravedad y sísmica de reflexión. Tesis doctoral, Facultad de ciencias exactas y naturales. Universidad de Buenos Aires.

Silvestro, J., & Zubiri, M. (2008). Convergencia oblicua: modelo estructural alternativo para la Dorsal Neuquina (39ºS)-Neuquén. *Revista de la Asociación Geológica Argentina*, *63*(1), 49-64.

Sinclair, H. (2012). Thrust wedge/foreland basin systems. *Tectonics of Sedimentary Basins: Recent Advances*, 522-537.

Spalletti, L.A., Veiga G.D., Schwarz, E. & Franzese J.R. (2008). Depósitos de flujos gravitacionales subácueos de sedimentación en el flanco active de la Cuenca Neuquina durante el Cretácico Temprano. *Revista de la Asociación Geológica Argentina, 63,* 442-453.

Spalletti, L.A., Franzese, J.R., Morel, E., D´Elia, L., Zúñiga, A., & Fanning, C.M. (2010). Consideraciones acerca de la sedimentología, paleobotánica y geocronología de la Formación Piedra del Águila (Jurásico Inferior, Neuquén, República Argentina). *Revista de la Asociación Geológica Argentina*, *66*, 305-313.

Spalletti, L.A., Veiga, G.D. & Schwarz, E. (2011). La Formación Agrio (Cretácico Temprano) en la Cuenca Neuquina. En *Geología y Recursos Naturales de la Provincia del Neuquén. Relatorio del XVIII Congreso Geológico Argentino* (pp. 145-160). Neuquén, Argentina.

Spalletti, L.A. (2013). Influencia del arco magmático protoandino en la acomodación sedimentaria, la fisiografía y las características de los depósitos del Jurásico Superior y Cretácico Inferior en la Cuenca Neuquina*. Anales Academia Nacional de Ciencias Exactas, Físicas y Naturales. 65,* 28-42.

Stipanicic, P.N. (1966). El Jurásico de la Vega de la Veranada (Neuquén), el Oxfordense y el diastrofismo divesiano (Agazziz-Yaila) en Argentina. *Revista de la Asociación Geológica Argentina, 20* (4), 403-478. Buenos Aires.

Stipanicic, P.N. & Rodrigo, F. (1968). The Jurassic and Neocomian diastrophism in Argentina and Chile. *XXII International Geological Congress*. Abstracts. Praga.

Thorne, J. A., & Watts, A. B. (1989). Quantitative analysis of North Sea subsidence. *AAPG Bulletin*, *73*(1), 88-116.

Turcotte, D. L. & Schubert, G. (2002). *Geodynamics*: *Applications of continuum physics to geological problems* 456 pp.

Uliana, M. A., Biddle, K. T. & Cerdan, J. (1989). Mesozoic Extension and the Formation of Argentine Sedimentary Basins: Chapter 39: Analogs.

Veiga, G.D., Schwarz, E. & Spalletti, L.A. (2011). Análisis estratigráfico de la Formación Lotena (Calloviano superior-Oxfordiano inferior) en la Cuenca Neuquina Central, República Argentina. Integración de información de afloramientos y subsuelo. *Andean Geology, 38*, 171-197.

Veiga, G. D., Schwarz, E., Spalletti, L. A. & Massaferro, J. L. (2013). Anatomy and Sequence Architecture of the Early Post-Rift in the Neuquén Basin (Argentina): A Response to Physiography and Relative Sea-Level Changes. *Journal of Sedimentary Research, 83*(8), 746-765.

Vergani, G., Tankard, A.J. Belotti, H.J. & Welsnik, H.J. (1995). Tectonic Evolution and Paleogeography of the Neuquén basin. En A.J. Tankard, R. Suárez Sorucco y H.J. Welsnik (Eds.). *Petroleum Basins of South America. American Association of Petroleum Geologists, Memoir*. 62, 383-402.

Vergani, G.D. (2005). Control estructural de la sedimentación jurásica (Grupo Cuyo) en la Dorsal de Huincul, Cuenca Neuquina. Modelo de falla lístrica rampa-plano invertida. *Boletín de Informaciones Petroleras, 1(1)*: 32-42.

Vergara, M., Levi, B., Nyström, J. O., & Cancino, A. (1995). Jurassic and Early Cretaceous island arc volcanism, extension, and subsidence in the Coast Range of central Chile. *Geological Society of America Bulletin*, *107*(12), 1427-1440.

Watkinson, M.P., Hart, M.B. & Joschi, A. (1977). Cretaceous Tectonostratigraphy and the Development of the Cauvery Basin, Southeast India, *Petroleum Geosciense, 13*, 181–191.

Watts, A.B. & Ryan, W.B.F. (1976). Flexure of the lithosphere and continental margin basins. En: M.H.P. Bott (ed.) *Sedimentary Basins of Continental Margins and Cratons*. *Tectonophysics*, *36*(l-3), 25-44.

704 Watts, A. B., Karner, G., & Steckler, M. S. (1982). Lithospheric flexure and the evolution of
705 sedimentary basins. *Philosophical Transactions of the Royal Society of London. Series*
706 *A, Mathematical and Physical Sciences*, *305*(1489), 249-281.

707 Watts, A.B. (2001) *Isostasy and Flexture of the Lithosphere*. Department of Earth Sciences,
708 Oxford University: Cambridge University Press.

709 Weaver, C. (1931). Paleontology of the Jurassic and Cretaceous of West Central Argentina.
710 *Universty of Washington. Memoir 1*, 1-469. Seattle.

711 Williams, K. E. (1995). Tectonic subsidence analysis and Paleozoic paleogeography of
712 Gondwana.

713 Xie, X. & Heller, P.L. (2009). Plate tectonics and basin subsidence history. *Geological Society*
714 *of America Bulletin*, *121,* 55–64.

715 Yrigoyen, M.R. (1991). Hydrocarbon resources of Argentina. In World Petroleum Congress,
716 No. 13. Petrotecnia, Special Issue: 38-54. Buenos Aires.

717 Zavala, C. (1993). *Estratigrafía y análisis de facies de la Formación Lajas (jurásico medio) en*
718 *el sector suroccidental de la Cuenca Neuquina. Provincia del Neuquén. República*
719 *Argentina*. (Tesis Doctoral). Departamento de Geología. Universidad Nacional del Sur.
720 Inédita.

721

722 **Figure captions**

723

724 **Figure 1**: Schematic map showing location, limits, major morphostructures and
725 study area of the Neuquén Basin. Modified of Howell et al. (2005).

726 **Figure 2**: Tectonic evolution of the Neuquén Basin. a) Rift stage: Mechanic subsidence
727 domain, isolated depocenters with siliciclastic, volcanic and volcaniclastic infill. b) Post-rift
728 stage. Thermal subsidence domain, connection of isolated depocenters, continental and
729 marine infill. c) Foreland stage. Flexural subsidence domain, fold and thrust belt develop and
730 continental infill. Based in Howell et al. (2005).

731 **Figure 3**: Location map showing study area (yellow rectangle), fold and thrust belt
732 region (orange) and major morphostructures.

733 **Figure 4**: Chronostratigraphy, tectonic evolution and major unconformities of the
734 Neuquén Basin. Based in Howell et al. (2005).

735 **Figure 5**: Location map of stratigraphic logs (yellow squares) and wells logs (red points) in
736 the study area.

737 **Figure 6**: The use of different values of palaeo-water depth (maximum = 100 m, minimum
738 = 0 m and mean = 50 m) and its influence on the calculated subsidence magnitude and
739 subsidence curves geometry. Example for the CG x-1 and PR x-1 wells.

740 **Figure 7**: Tectonic subsidence curves for wells for: a) ADP x-3, AN x-2, BEH x-2,
741 BjDC x-1, BSPe-4, Cam-18 and CCN. b) BSP e-4, CG x-1, CuC x-1, EPn x-1, EPS x-
742 1, CMN x-1. c) CCS, ChBS x-1, ChC x-1, CLN x-1, CoN e-3 and CoNS x-1. d) Pb x-1,

743 LPe x-2, Emo x-1, EP x-3, ETe x-1 and GN x-1. e) ECh x-1, EI x-1, Reyes S, LED x-2,
744 LRm X-1 and P x-2. f) LB x-2, P x-3, PBN xp-11, PCa x-1, PM-36 and PR x-1.

745 **Figure 8**: Tectonic subsidence curve calculated for the CG-x1 well (black line),
746 differences respect to the theoretical subsidence curve for an extensional basin
747 (dotted red line) and intervals considered for its description.

748 **Figure 9**: Flexural subsidence calculated using loads of 500, 1000 and 1500
749 meters height and density of 2700 kg/m³ over a lithosphere with a) Te = 5 km, b)
750 Te = 10 km and c) Te = 25 km; and its effect in the study area.

751 **Figure 10**: Dynamic subsidence calculated using different parameters and its
752 theoretical values to the study area.

753 **Table captions**

754

755 **Table 1**. Superficial porosity, compaction coefficient and density values. From
756 Sclater & Christie (1980) and Sawyer et al. (1982).

757 **Table 2**. Bathymetry values used for each lithostratigraphic unit.

758

759 **Table 3**. Base and top ages used for each lithostratigraphic unit in the study area.

760

Lithology	Superficial porosity (%)	c ($km^{-}1$)	Density (kg/m^3)
Clay	63	0.51	2720
Sand	49	0.27	2650
Gypsum	70	0.71	2710
Wackes	25.6	0.39	2680
Limestone	45	0.54	2700

Table 1. Superficial porosity, compaction coefficient and density values. From Sclater & Christie (1980) and Sawyer et al. (1982).

Formation/Group	Mean Bathymetry (m)	Min. Bathymetry (m)	Max. Bathymetry (m)
Tordillo Fm.	0	0	0
Auquilco Fm.	5	0	10
La Manga Fm.	10	0	20
Lotena Fm.	25	0	50
Cuyo Gr. (shallow facies)	25	0	50
Cuyo Gr. (deep facies)	75	50	100
Precuyano	0	0	0

Table 2. Bathymetry values used for each lithostratigraphic unit.

Unit	Interval	Age (My)	
		Base	Top
Tordillo Fm.	Kimmerdigian - Tithonian	153	144
Auquilco Fm.	Late Oxfordian	157	153
La Manga Fm.	Early to middle Oxfordian	159	157
Lotena Fm.	Middle Callovian	164.6	159
Cuyo Gr.	Hettangian / Sinemurian – Middle Callovian	190	164.6
Precuyano Cy.	Upper Triassic / Hettangian / Sinemurian	200	190

Table 3. Base and top ages used for each lithostratigraphic unit in the study area.

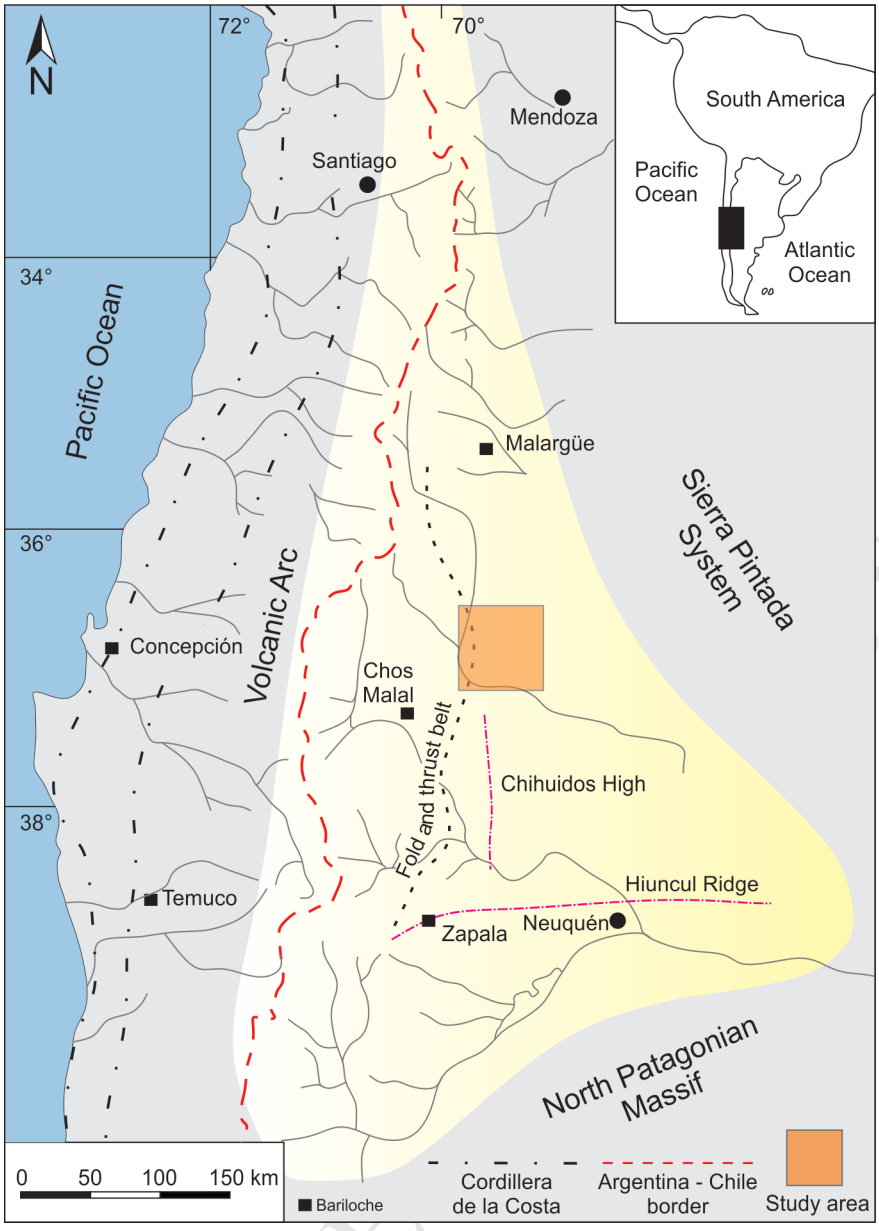
N
72°
70°
34°
36°
38°
Pacific Ocean
Mendoza
Santiago
South America
Pacific Ocean
Atlantic Ocean
Malargüe
Sierra Pintada System
Volcanic Arc
Concepción
Chos Malal
Fold and thrust belt
Chihuidos High
Hiuncul Ridge
Temuco
Zapala
Neuquén
North Patagonian Massif
0 50 100 150 km
Bariloche
Cordillera de la Costa
Argentina - Chile border
Study area

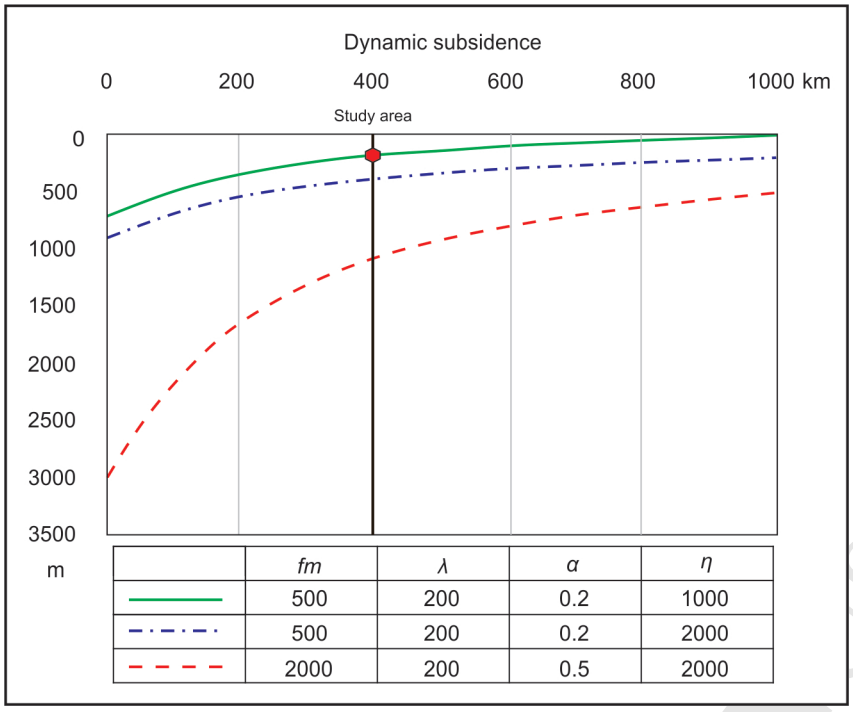

	fm	*λ*	*α*	*η*
———	500	200	0.2	1000
-·-·-	500	200	0.2	2000
– – –	2000	200	0.5	2000

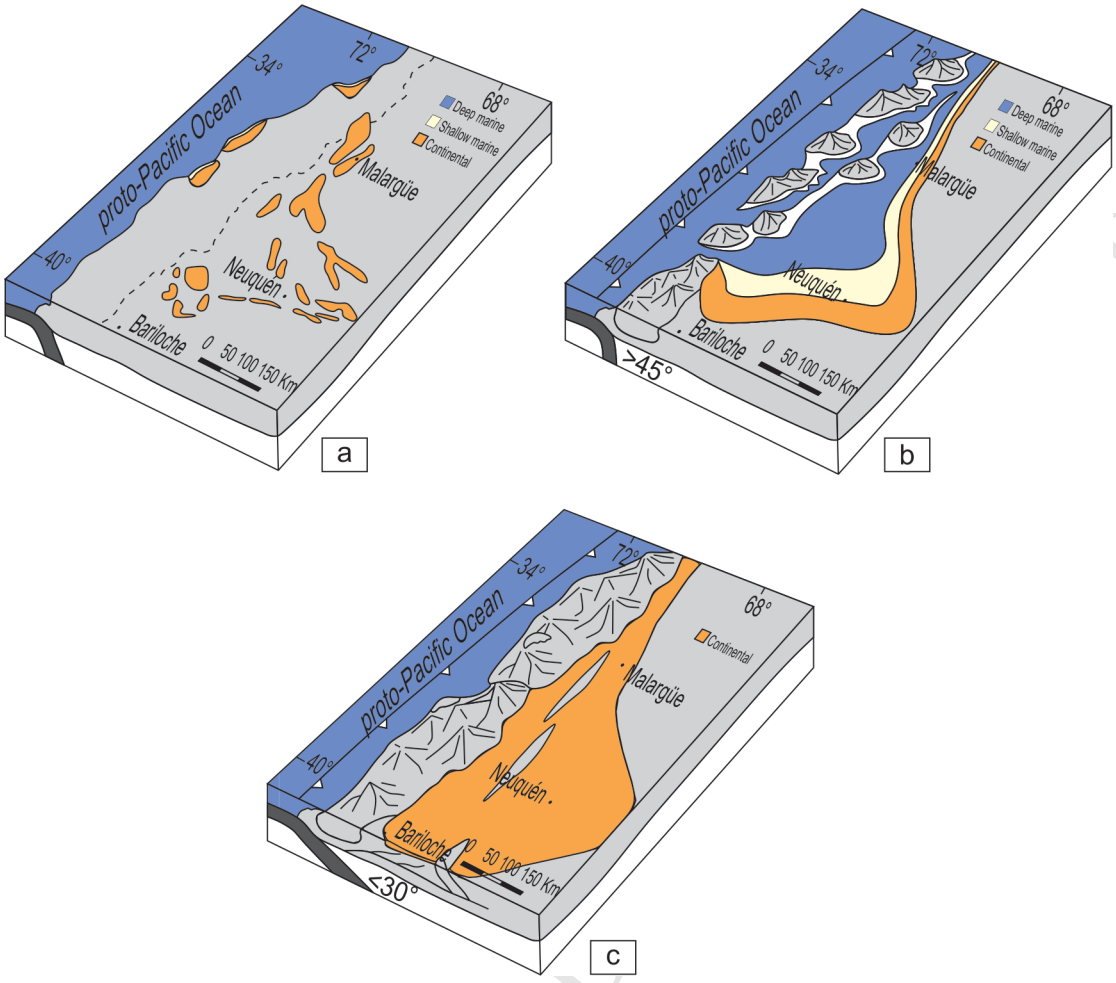

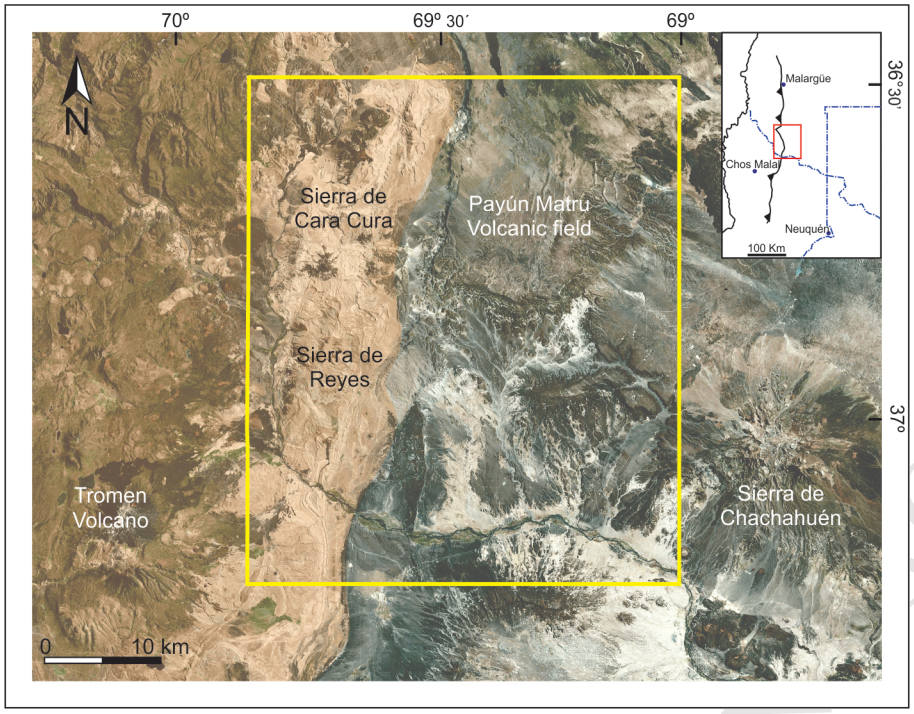

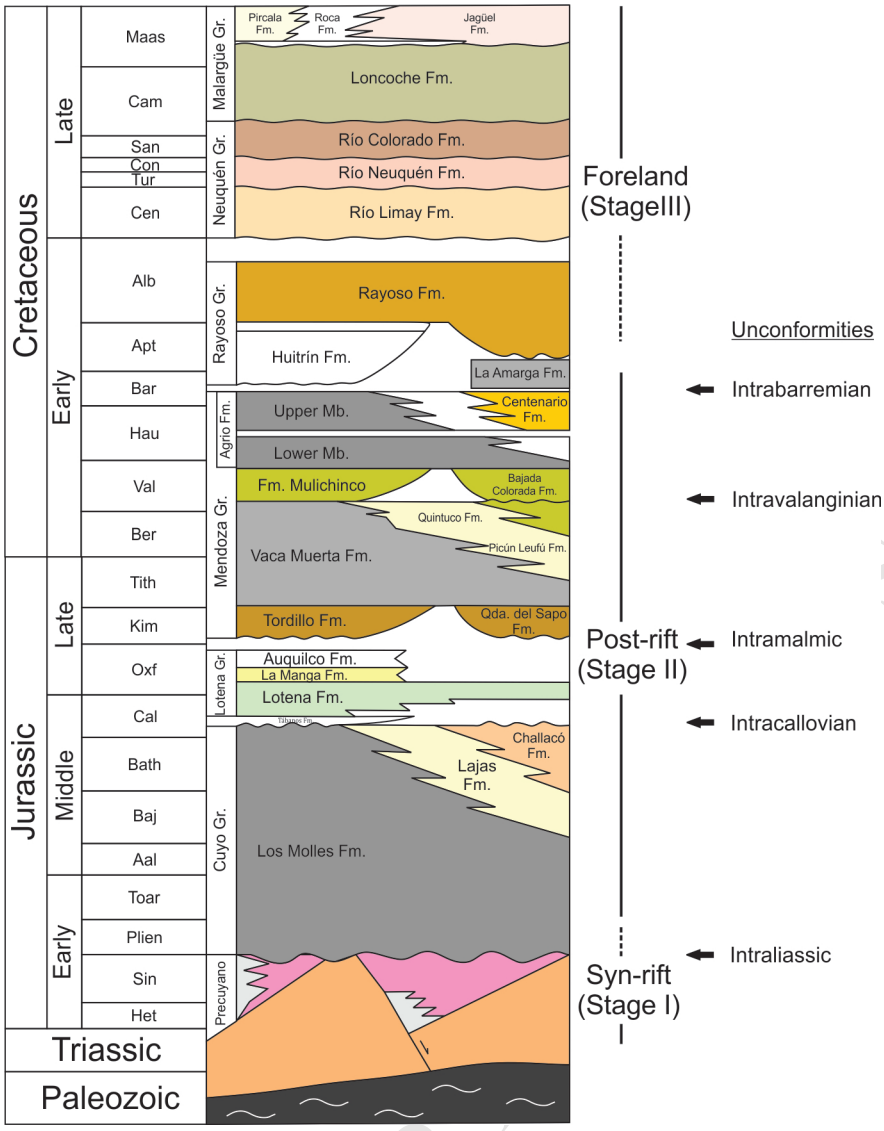

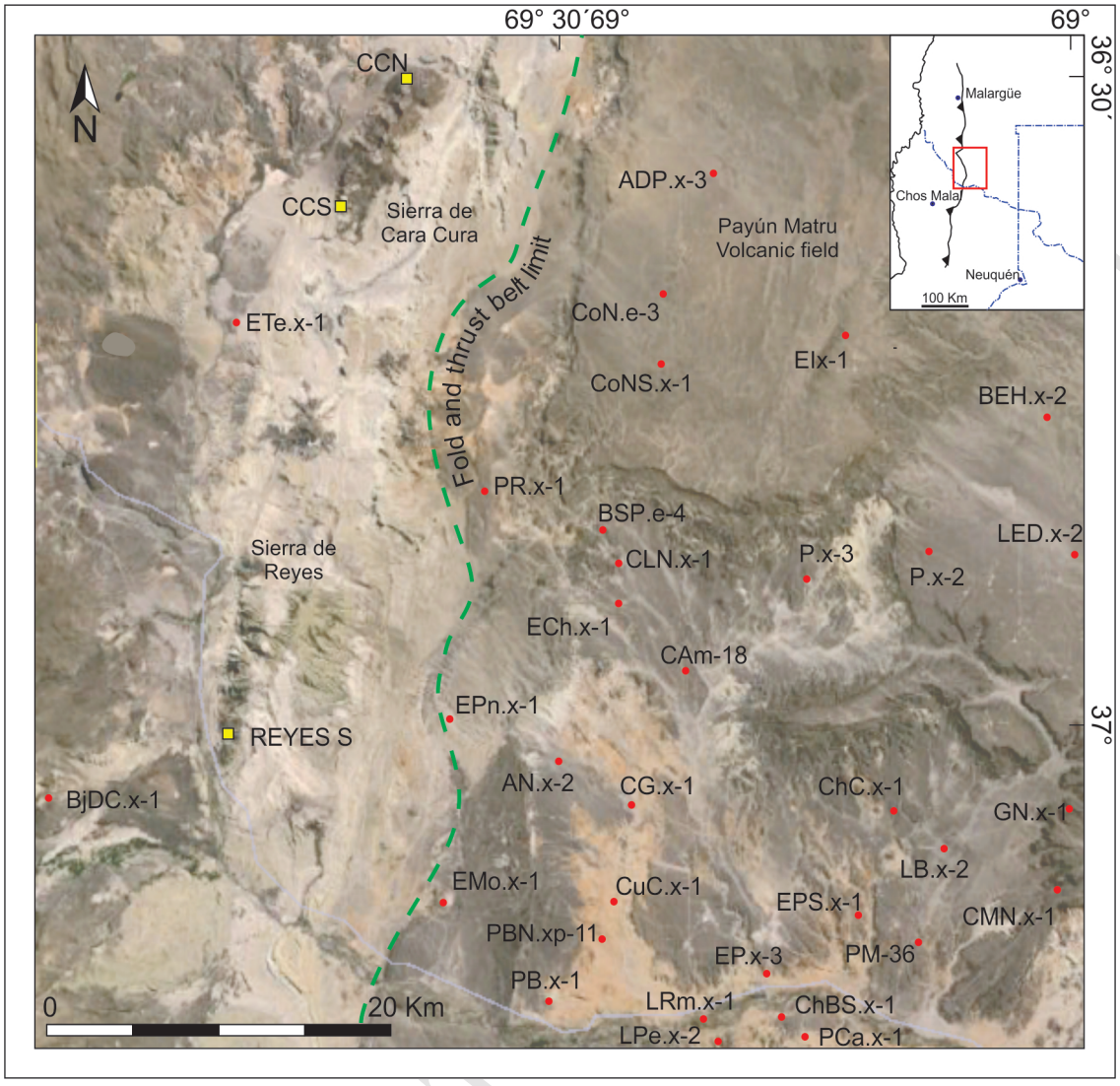
69° 30´69°
69°
36° 30´
37°
N
CCN
CCS
Sierra de
Cara Cura
ADP.x-3
Payún Matru
Volcanic field
Fold and thrust belt limit
ETe.x-1
CoN.e-3
CoNS.x-1
EIx-1
BEH.x-2
PR.x-1
BSP.e-4
LED.x-2
Sierra de
Reyes
CLN.x-1
P.x-3
P.x-2
ECh.x-1
CAm-18
EPn.x-1
REYES S
BjDC.x-1
AN.x-2
CG.x-1
ChC.x-1
GN.x-1
LB.x-2
EMo.x-1
CuC.x-1
EPS.x-1
CMN.x-1
PBN.xp-11
EP.x-3
PM-36
PB.x-1
LRm.x-1
ChBS.x-1
LPe.x-2
PCa.x-1
0
20 Km
Malargüe
Chos Malal
Neuquén
100 Km

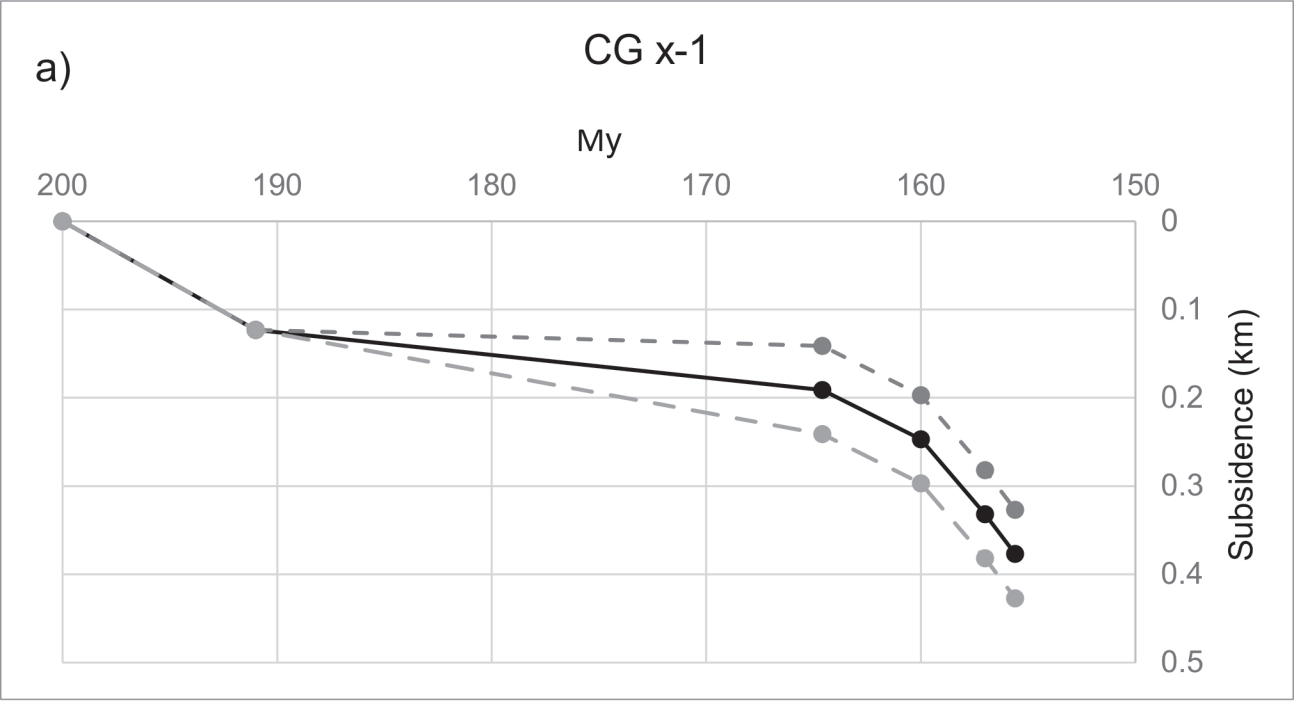
a)
CG x-1
My
200
190
180
170
160
150
0
0.1
0.2
0.3
0.4
0.5
Subsidence (km)

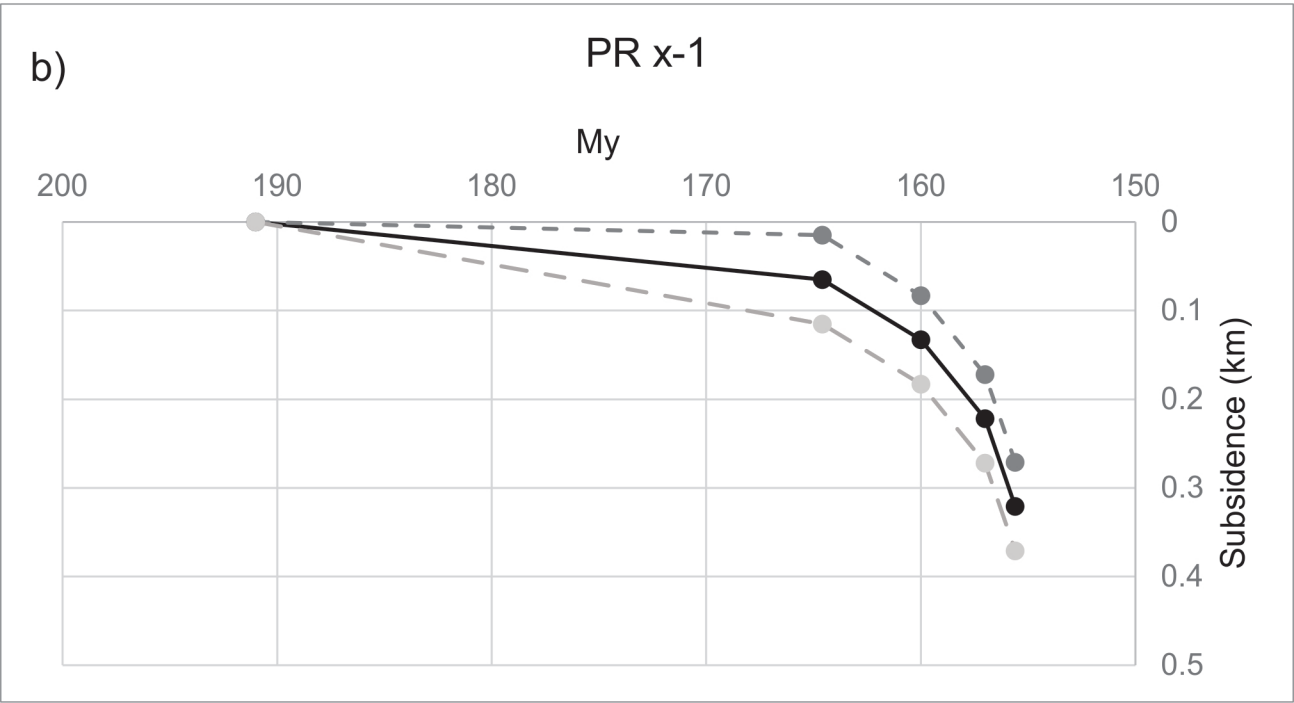
b)
PR x-1
My
200
190
180
170
160
150
0
0.1
0.2
0.3
0.4
0.5
Subsidence (km)

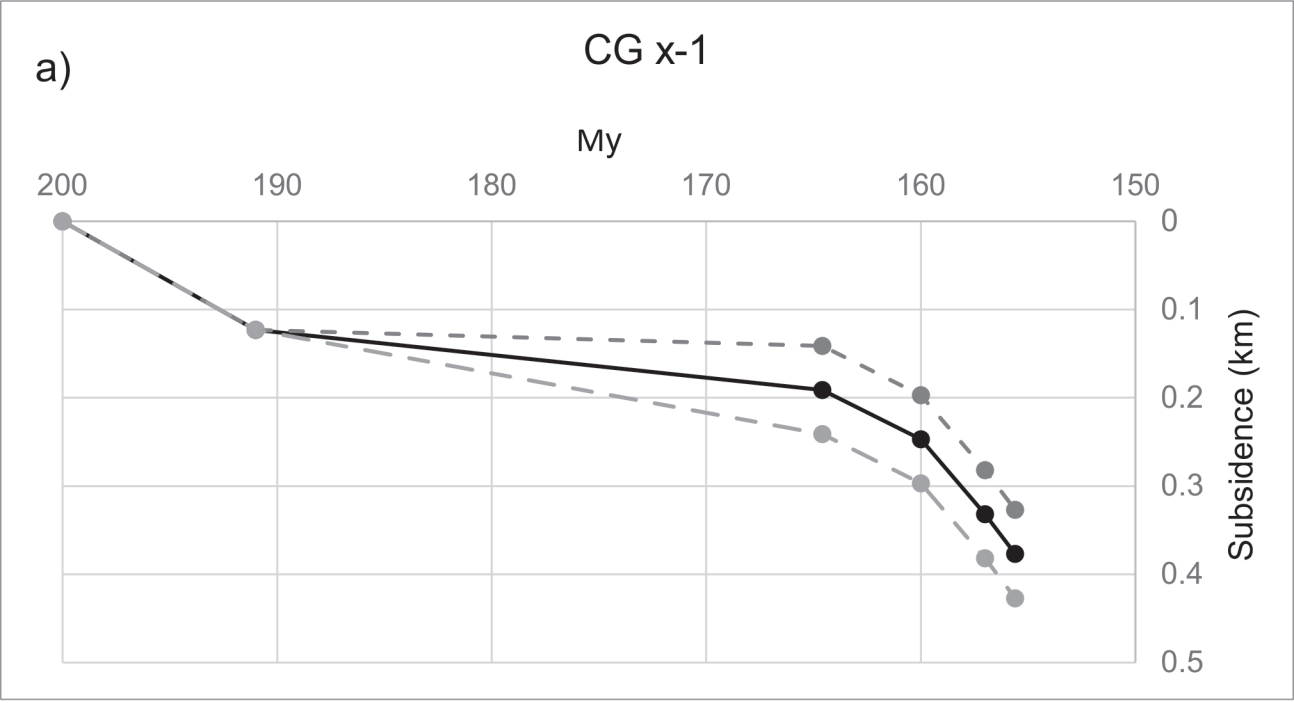
a)
CG x-1
My
200
190
180
170
160
150
0
0.1
0.2
0.3
0.4
0.5
Subsidence (km)

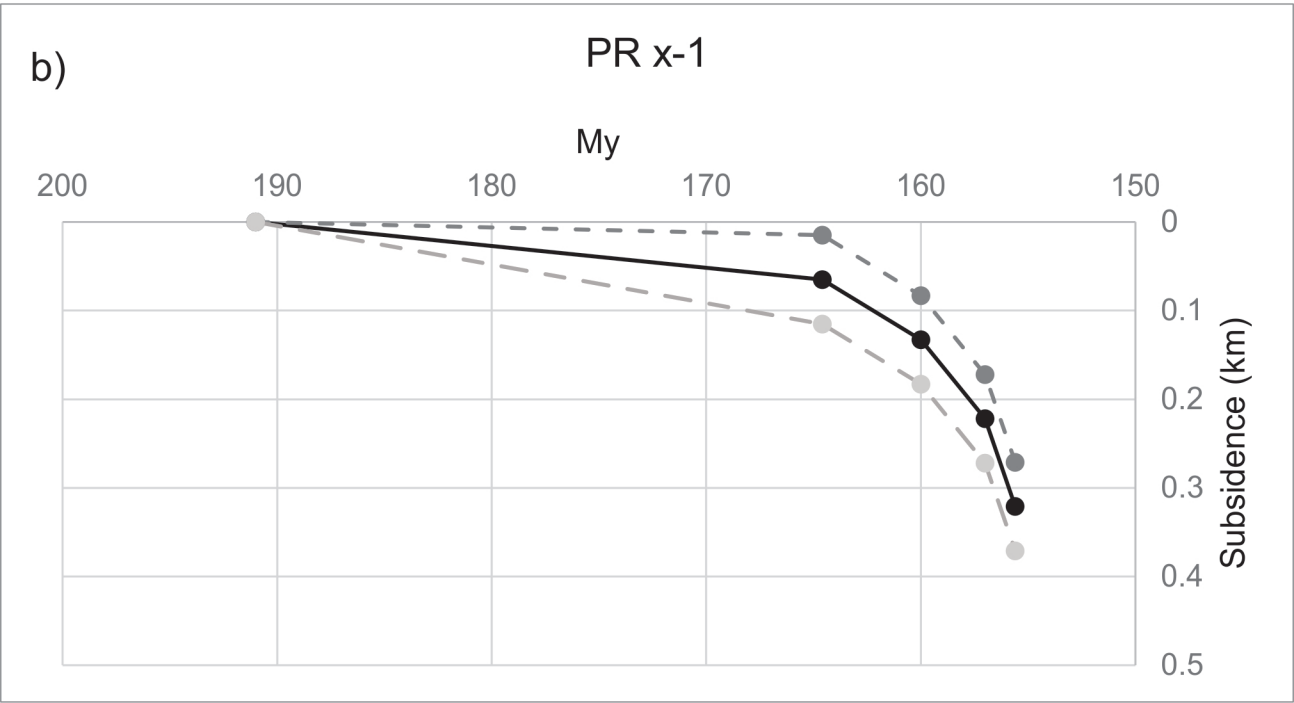
b)
PR x-1
My
200
190
180
170
160
150
0
0.1
0.2
0.3
0.4
0.5
Subsidence (km)

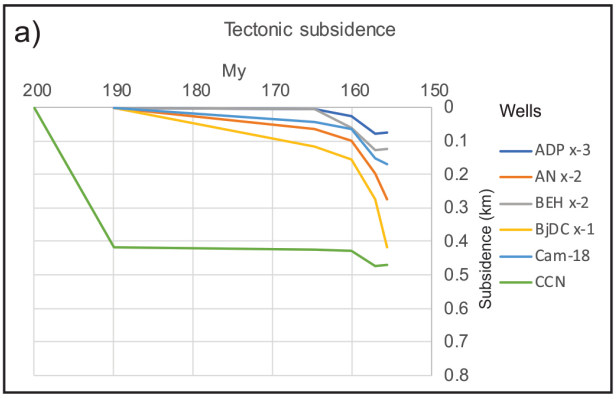
a)
Tectonic subsidence
My
200 190 180 170 160 150
0 0.1 0.2 0.3 0.4 0.5 0.6 0.7 0.8
Subsidence (km)
Wells
ADP x-3
AN x-2
BEH x-2
BjDC x-1
Cam-18
CCN

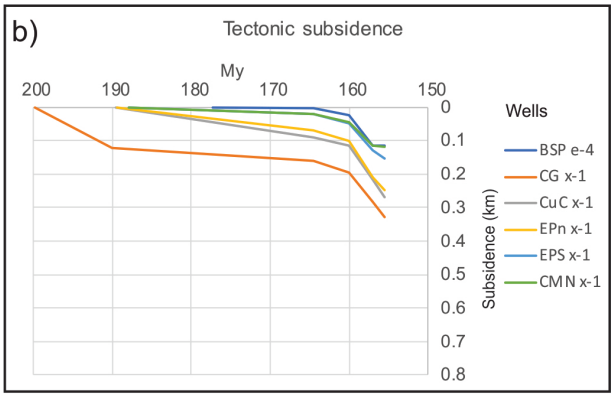
b)
Tectonic subsidence
My
200 190 180 170 160 150
0 0.1 0.2 0.3 0.4 0.5 0.6 0.7 0.8
Subsidence (km)
Wells
BSP e-4
CG x-1
CuC x-1
EPn x-1
EPS x-1
CMN x-1

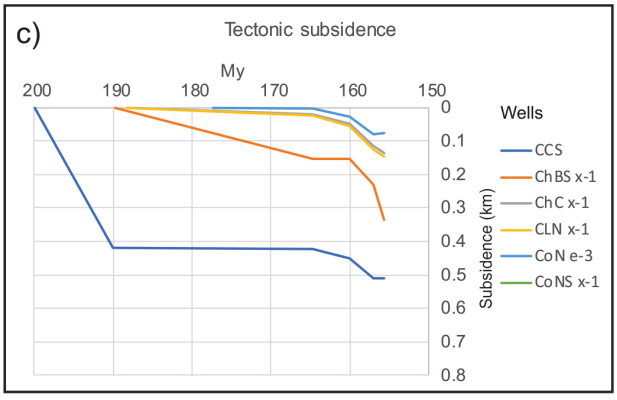
c)
Tectonic subsidence
My
200 190 180 170 160 150
0 0.1 0.2 0.3 0.4 0.5 0.6 0.7 0.8
Subsidence (km)
Wells
CCS
ChBS x-1
ChC x-1
CLN x-1
CoN e-3
CoNS x-1

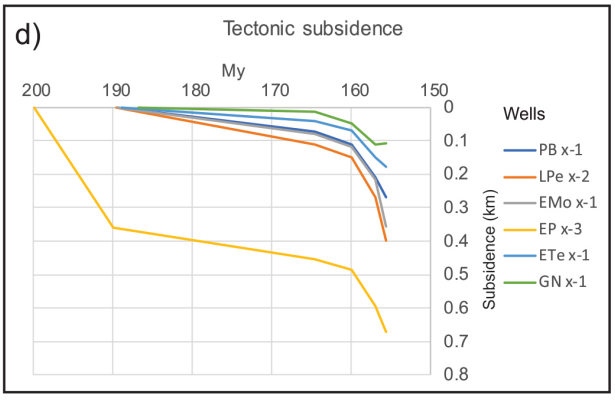
d)
Tectonic subsidence
My
200 190 180 170 160 150
0 0.1 0.2 0.3 0.4 0.5 0.6 0.7 0.8
Subsidence (km)
Wells
PB x-1
LPe x-2
EMo x-1
EP x-3
ETe x-1
GN x-1

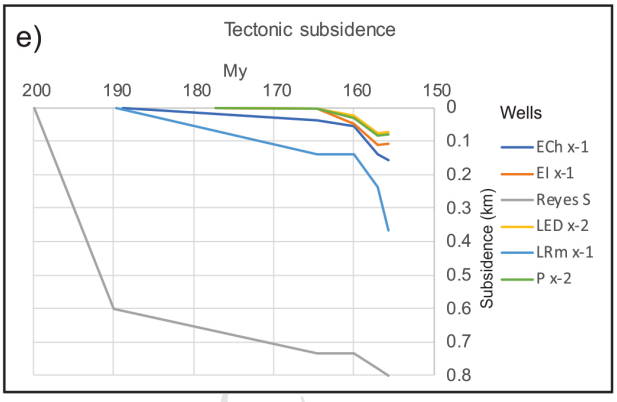
e)
Tectonic subsidence
My
200 190 180 170 160 150
0 0.1 0.2 0.3 0.4 0.5 0.6 0.7 0.8
Subsidence (km)
Wells
ECh x-1
El x-1
Reyes S
LED x-2
LRm x-1
P x-2

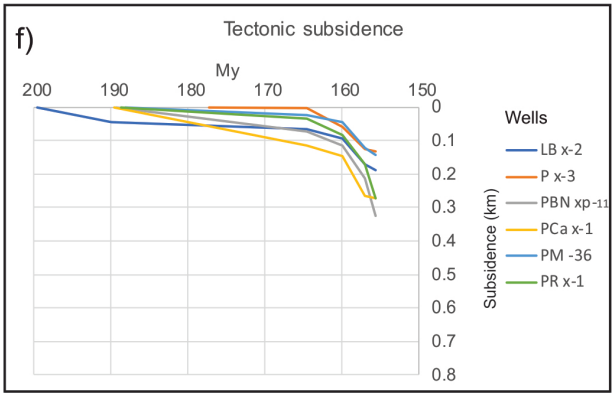
f)
Tectonic subsidence
My
200 190 180 170 160 150
0 0.1 0.2 0.3 0.4 0.5 0.6 0.7 0.8
Subsidence (km)
Wells
LB x-2
P x-3
PBN xp-11
PCa x-1
PM -36
PR x-1

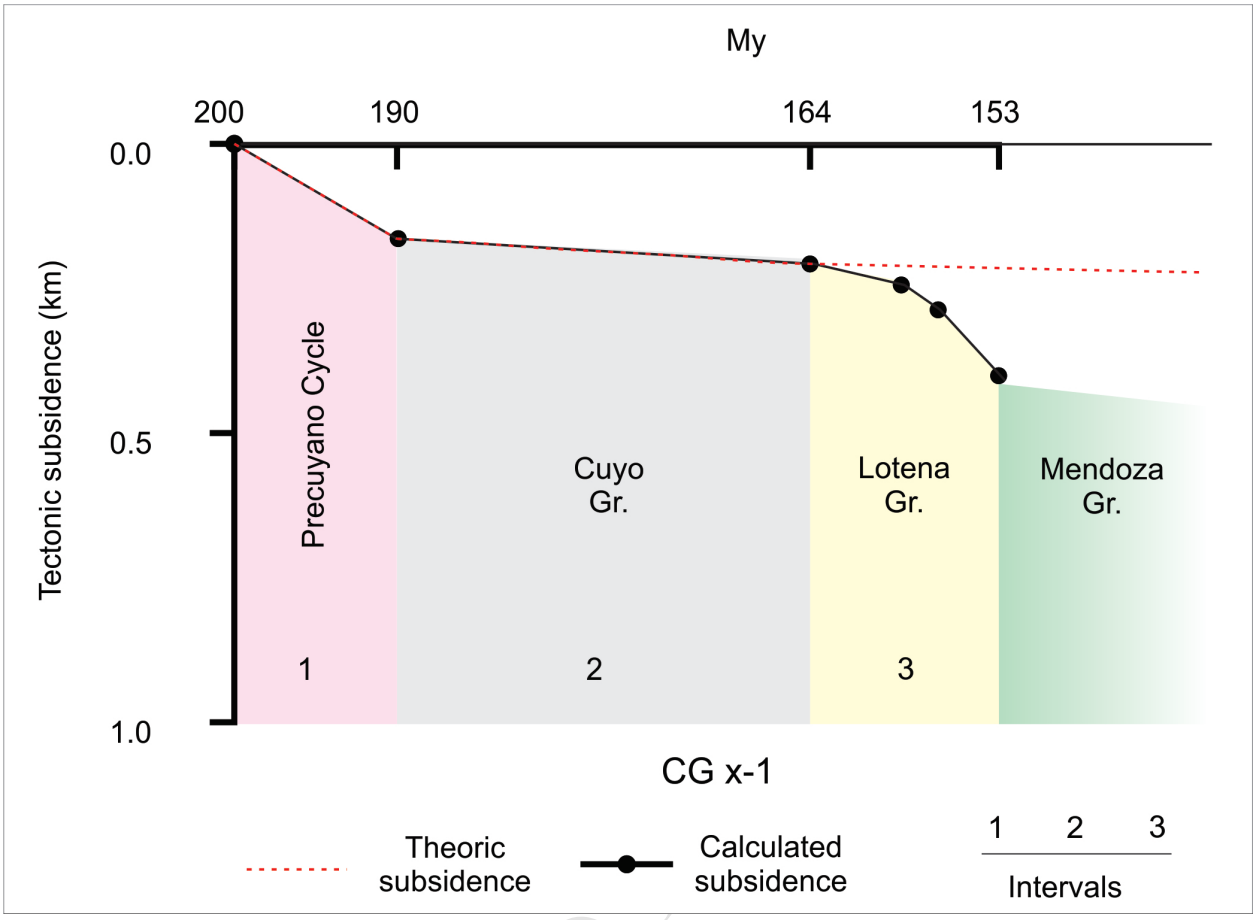

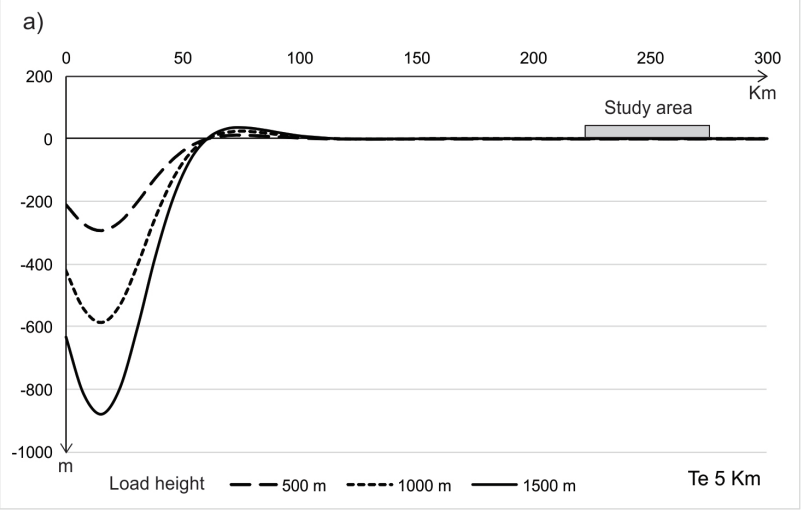
a)
0
50
100
150
200
250
300
200
Km
Study area
0
-200
-400
-600
-800
-1000
m
Load height
500 m
1000 m
1500 m
Te 5 Km

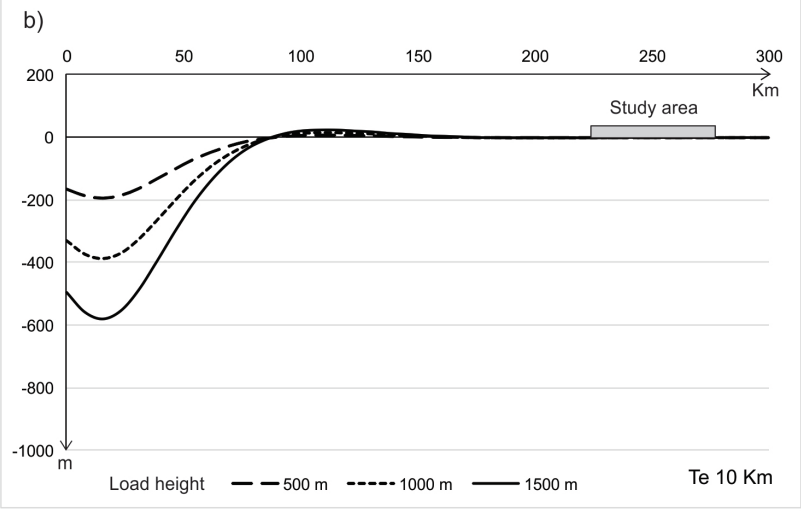
b)
0
50
100
150
200
250
300
200
Km
Study area
0
-200
-400
-600
-800
-1000
m
Load height
500 m
1000 m
1500 m
Te 10 Km

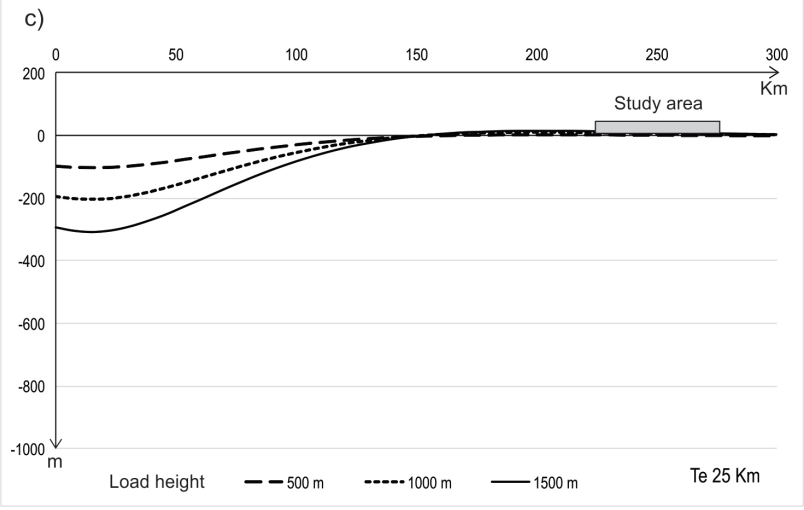
c)
0
50
100
150
200
250
300
200
Km
Study area
0
-200
-400
-600
-800
-1000
m
Load height
500 m
1000 m
1500 m
Te 25 Km

Highlights

Backstripping was applied for Late Triassic - Late Jurassic period of Neuquén Basin.

Obtained tectonic subsidence curves differs from thermal subsidence models.

The accumulation of Lotena Group could have been controlled by dynamic subsidence.